AFRL-SR-AR-TR-08-0522

REPORT DOCUMENTATION PAGE

1. AGENCY USE ONLY (*Leave Blank*)	2. REPORT DATE	3. REPORT TYPE AND DATES COVERED
	Dec, 2008	Final Technical, 01/04/05 – 10/31/08

4. TITLE AND SUBTITLE
Application of Advanced Concepts and Techniques in Electromagnetic Topology Based Simulations: CRIPTE and Related Codes

5. FUNDING NUMBERS
FA9550-05-1-0323

6. AUTHORS
Naz E. Islam

7. PERFORMING ORGANIZATION NAME(S) AND ADDRESS(ES)
University of Missouri-Columbia
Department of Electrical and Computer Engineering
Columbia, MO, 65211

8. PERFORMING ORGANIZATION REPORT NUMBER

9. SPONSORING / MONITORING AGENCY NAME(S) AND ADDRESS(ES)
AFOSR/NE
875 North Randolph Street, Suite 325
Arlington, VA 22203

10. SPONSORING / MONITORING AGENCY REPORT NUMBER

11. SUPPLEMENTARY NOTES

12a. DISTRIBUTION / AVAILABILITY STATEMENT
Unlimited

12b. DISTRIBUTION CODE
AFOSR/NE

13. ABSTRACT *(Maximum 200 words)*

This final technical report reviews our research activities during the period of this grant with an emphasis on some of the main finding during the research period. The key finding of our study is that the Electromagnetic Topology (EMT) simulation method is a viable option for analyzing the response of large electrical systems that are subjected to external electromagnetic fields. Simulations using a EMT domain code, CRIPTE, that was developed for AFRL/NM by the French defense contractor, ONERA, indicate that this simulation method can be applied to wave-aperture interactions, cable coupling, field penetration through apertures, field twisted pair interactions and many other known interaction phenomena. Since the EMT method does not require a simultaneous analysis of an entire geometry, but can be analyzed in a modular fashion, EMT techniques can be used to simulate the response of very large electrical systems. Simulations using the EMT code were verified through experiments in the Anechoic Chamber at the high power electromagnetic laboratory (HiPER) at the University of Missouri, Columbia. .

14. SUBJECT TERMS	15. NUMBER OF PAGES
Electromagnetic Topology, Modeling, Cross-talk, Aperture interactions, BLTequations	41
	16. PRICE CODE

17. SECURITY CLASSIFICATION OF REPORT	18. SECURITY CLASSIFICATION OF THIS PAGE	19. SECURITY CLASSIFICATION OF ABSTRACT	20. LIMITATION OF ABSTRACT
Unclassified	Unclassified	Unclassified	None

UNIVERSITY OF MISSOURI
College of Engineering

Electrical and Computer Engineering

"Application of Advanced Concepts and Techniques in Electromagnetic Topology Based Simulations: Cripte and Related Codes"

Final Technical Report
1 April 2006 – 31 October 2008

AFOSR Grant FA9550-05-1-0323

Submitted by:

Naz E. Islam — Principal Investigator and Professor
Department of Electrical and Computer Engineering
University of Columbia
Columbia, MO 65211
Tel. (573) 882-7570
Fax (573) 882-0397
e-mail: islamn@missouri.edu

TABLE OF CONTENTS

I. INTRODUCTION

This report summarizes our research work for the duration of the AFOSR Grant F49620-02-1-0183, specifically covering the last reporting period. This report highlights some of the achievements and covers both our theoretical analysis as well as experiments to demonstrate the concept of applying Electromagnetic Topology (EMT) techniques to analyze the response of large electrical systems under external electromagnetic radiation. The project objective was to study the feasibility of applying EMT with the CRIPTE code. This study has resulted in the publication of more than 15 journal papers and book articles in the area of EMT simulations, and was presented in more than 25 conferences as well as special sessions.

The CRIPTE code is based on the EMT theory initially presented by AFRL, NM, and was designed to study the response of very large electrical systems in an electromagnetic environment. The EMT code relies on computations through multi-conductor transmission line network and is therefore convenient for the analysis of very large electrical systems where the conventional codes capabilities become limited. The networks defined through the code consist of cable lines (tubes) connected through junctions. The junctions here represent computers or any other component of the system. The measured S-parameters, or its equivalent computed values, are then fed into the junctions as input. The code thus analyzes the network which has been 'volume decomposed' into junctions and tubes. RF effects are simulated by introducing external RF sources on the cable network. This initial analysis for a given section of a large system is building block upon which the rest of the system is analyzed.

In this final report we briefly discuss a number of scenarios using the CRIPTE code. We have also highlighted some of the major issues that need to be tackled using the code and have introduced new concepts for aperture interaction with electromagnetic fields, which has been verified with experiments. Some of the concepts discussed include aperture interactions, analyzed CAT-5 cables and twisted pairs and a host of other simulations, some verified through experiments in our lab. A close collaboration was also established with DEHE/AFRL, NM, while faculties at MU and UNM also assisted in our discussions. Our collaborative work with AFRL/NM has been presented at classified sessions, that includes the Five-power (US, UK, Germany, France and Italy) Air Senior National Representative (ASNR) High Power Microwave Meeting, February 2005 at Eglin AFB, FL, and the Directed Energy Professional Society (DEPS) High Power Microwave Conference, in August 2004 in Albuquerque.

Besides establishing the simulation laboratory and the experimental setup using an Anechoic Chamber, we have added in-house developed tools for analysis and experiments. This includes a GHz TEM cells as well as a large Helmholtz's Coil for interaction studies as well as an in-house FDTD code to aid our analysis. A number of researches including US nationals have contributed to the research effort at both UMC and AFRL.

Understanding the effects of EMP on systems and devices is expected to lead to predictive capabilities, which will ultimately in shielding studies against such effects. The research effort has also resulted in a number of journal and conference publications and interactions with peers and DoD personnel conducting research in this area.

II. SUMMARY OF EMT THEORY

For large electrical systems, the EMT solution method offers a strategy to handle the complexities associated with electrical wiring in systems. The first and most important aspect of EMT is the assumption that volumes can be decomposed into subvolumes that can interact with each other through 'preferred path' such as apertures and cables. The assumption is based on the premise that there is enough shielding between volumes and there is no energy transfer through shielding. The topological networks that result in an EMT circuit are essentially composed of junctions, tubes, and sources. Junctions are elements that terminate or connect transmission lines. Common types of junctions are open-circuited, short-circuited, 50-ohm, and matched loads. Another example of junctions is an n-port device that can be defined by scattering parameters or similar parameters. Tubes represent the connections between junctions and can be defined by transmission line per unit values. Parameters from junctions and tubes can be derived from formulas, tables, measured values, or the results of full-wave analysis. Sources can either be voltage sources or current sources.

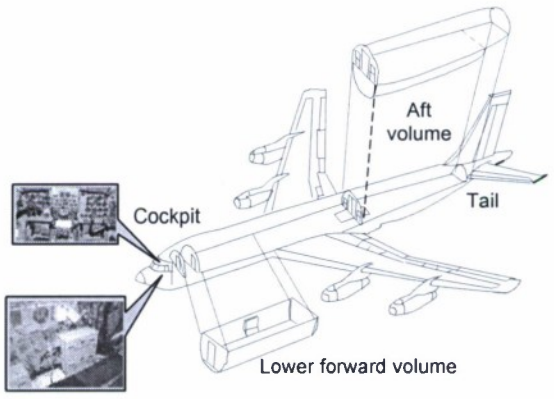

Figure 1 Volume decomposition diagram. The entire system is topologically broken down into different volumes.

Consider a large electrical system such as an aircraft shown in Fig 1. Assume that the entire system can be decomposed into sub-volumes, the aircraft in Fig. 1, for example, can be decomposed into such volumes as cockpit, lower forward, wing, tail, and aft volumes that can interact with each other through an interaction path such as apertures and cables. Inside the cockpit, there basically exist delicate electronic circuits and wiring cables as main constituents of the electrical system of the aircraft. The topological networks that represent the system interactions are essentially composed of junctions and tubes. Junctions that represent volumes are elements that terminate or connect transmission lines. Tubes represent the connections between junctions and can be defined by transmission line per unit parameters. Inputs for junctions and tubes can be derived from formulas, tables, measured values, or simulated results. Fig. 2 shows the diagram of the topological network of the aircraft shown in Fig. 1. There are 5 main junctions and 4 tubes that form the upper-level network consisting of the cockpit, the wing, the fuselage, and the tail. There exists inside the cockpit junction the lower-level network of the electronic circuits and cable wirings.

For topological network equations, consider a simplified sub-component of the large electrical system. Fig 3 below shows two PCs in a subsystem that is represented by two circular junctions connected by a tube-like structure. At the junction of E_2, vectors for both the incoming ($W_1(L)$) and outgoing waves ($W_2(0)$) are related by the junction scattering matrix (S_{12}) through the scattering equation, expressed as

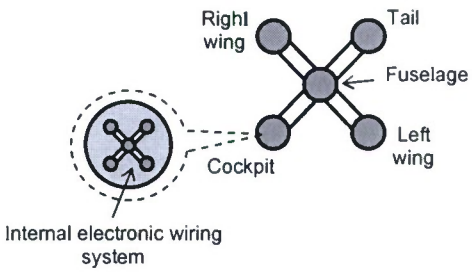

Figure 2 Topological network consisting of the external and internal levels, included within each other.

$$(W_2(0)) = (S_{12})(W_1(L)) \qquad \textbf{(1)}$$

For multiconductor lines, the incoming and outgoing waves at the junction of E2 can be represented, respectively, by (V)+(Zc)(I) and (V)-(Zc))(I) where (V) and (I) are voltages and currents at each port of the junction and Zc is the characteristic impedance. The scattering parameter (S) can be written in terms of the admittance matrix (Y) as in equation (2), with the characteristic impedance matrix at the junction of E_2 with N_1 conductors along tubes is represented through equation (3):

$$(S) = [(1) - (Z_c)(Y)][(1) + (Z_c)(Y)]^{-1} \qquad (2)$$

$$(Z_c) = \begin{pmatrix} Z_{c1,1} & \cdots & Z_{c1,N1} \\ \vdots & \ddots & \vdots \\ Z_{cN1,1} & \cdots & Z_{cN1,N1} \end{pmatrix} \qquad (3)$$

Propagation of the incoming and outgoing waves, along the tube in the opposite directions with an equivalent distributed source (Ws), can be characterized by a propagation matrix (Γ). The resulting propagation equation becomes

$$(W_1(L)) = (\Gamma)(W_1(0)) + (Ws) \qquad (4)$$

Signals on an entire transmission-line network is expressed through the BLT (Baum Liu and Tesche) equation which is in essence, the multiconductor transmission line (MTL) network composed of the incoming wave vector, the outgoing wave vector, and the source wave super vector, respectively, shown above as [W(0)], [W(L)], and [Ws]. The network scattering and propagation super matrices are represented, respectively, by [S] and [Γ]. Using the supervector and supermatrix forms seen in (1) and (4), the BLT equation can be expressed as

$$\{[I] - [S][\Gamma]\}[W(0)] = [S][Ws], \qquad (5)$$

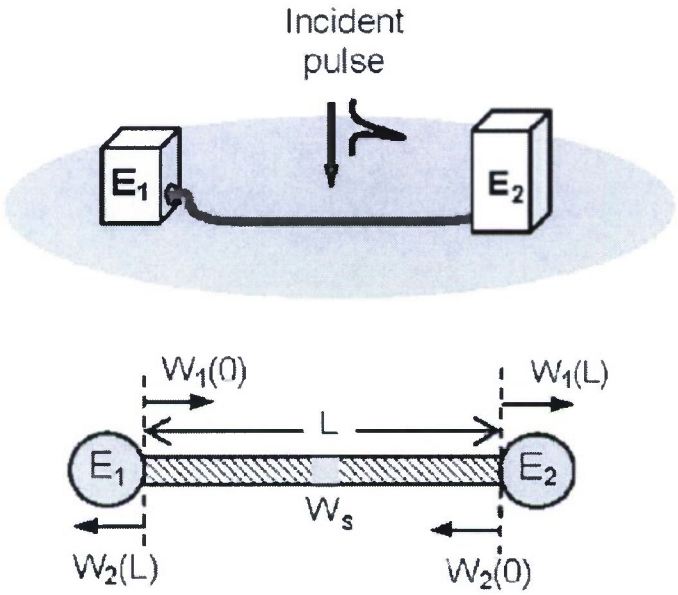

Figure 3

where [I] is the identity super matrix. Solutions of the BLT equations have been incorporated into an electromagnetic topological code.

III. SUMMARY OF SIMULATION AND EXPERIMENTAL LAB SETUP

A simulation and experimental laboratory (High Power Electromagnetic Radiation HiPER), was setup for the simulation and experimental analysis for the validation of CRIPTE code at UMC. Our effort has contributed significantly to the understanding of topological schemes, specifically for aperture interactions, cable interactions, cross talk and the usage of the compaction scheme as shown through the CRIPTE code. The results were published and documented for use at DE/AFRL, NM.

Basic Simulation Codes The basic components of the codes include RORQUAL, LAPLACE and CRIPTE, that were installed on a LINUX server (RedHat 9.0, Dell Xeon) and two independently running workstations (WINXP, Dell Pentium 4) on LAN network. RORQUAL is the software allows the user to execute numurical operations on both real and complex signals on Time and Frequency domains. Many features are available such as basic operations, Fourier Transform, inverse Fourier Transformer, Fast Fourier Transform, inverse Fast Fourier Transform, etc. while LAPLACE is a numerical code, which handles the calculation of a multiconductor transmission line's impedance and admittance. The LAPLACE code solves by using the Method of Moments on the cross sectional geometry of the cable harnesses and the dielectric materials surrounding the cable conductors. The CRIPTE simulation tool is the key to study the RF system interactions. By characterizing the tubes (cable parameters) using the output from the LAPLACE code and junctions from CRIPTE itself (impedance parameters) or measurement (S-parameters), the interaction can be performed. In the initial stages, the high power radiation code (HEIMDALL) code was used in the analysis but later abandoned since it was not as effective in collaborating CRIPTE results as anticipated.

In-House Simulations for Comparisons (FDTD) In order to compare results with EMT based simulations, source generation, compare transfer function generation results at the aperture, we developed a finite-difference time-domain (FDTD) code in-house. Both the FDTD and the EMT simulations were carried out on a Pentium XEON-processor Linux server. The 2D and 3D FDTD codes were implemented using the C program language.

Anechoic Chamber A test anechoic chamber was added to the project from a supplement grant from AFOSR. The system will enable the researchers to perform an electromagnetic conducted and radiation susceptibility tests on cables and equipment under test and has enhanced the research capability to support the existing DOD programs at the RF Effect laboratory at the University of Missouri-Columbia. A near field probe, a network analyzer (borrowed from another group) has also been added

Trainings Facility The HiPER laboratory, at MU is now the prime training facility for graduate and under graduate students for 'effects' studies and provides the knowledge and skills necessary to work in US laboratories and the industry.

IV. SUMMARY: TRANSFER FUNCTION GENERATION IN EMT SIMULATIONS

Our initial effort in the validation of the CRIPTE code was to generate models for external-internal interactions through apertures and verify the results with FDTD analysis for aperture interactions.

Topological Approach (Introduction of Transfer Function) A new concept was introduced in the simulation tool where the external-internal interactions were treated through topological decomposition and a transfer function was generated into the simulation sequence through simulations. This was previously done through experiments. Such a scheme produced results that are consistent with experiments. In future CRIPTE simulations generated transfer function can be used in different interaction sequences and thus will not require a separate set of experiments for its generation. The transfer function was generated using a series of algorithm in EMT volume decomposition, external field couplings, field penetration through openings, and internal cable propagation of induced signals through computer network analysis.

An schematic involving an aircraft system with a penetration path (aperture) consisting of two computer mainframes, connecting each other with a communication cable was used in the validation setup. The transfer function schematic is shown in Fig TF-1

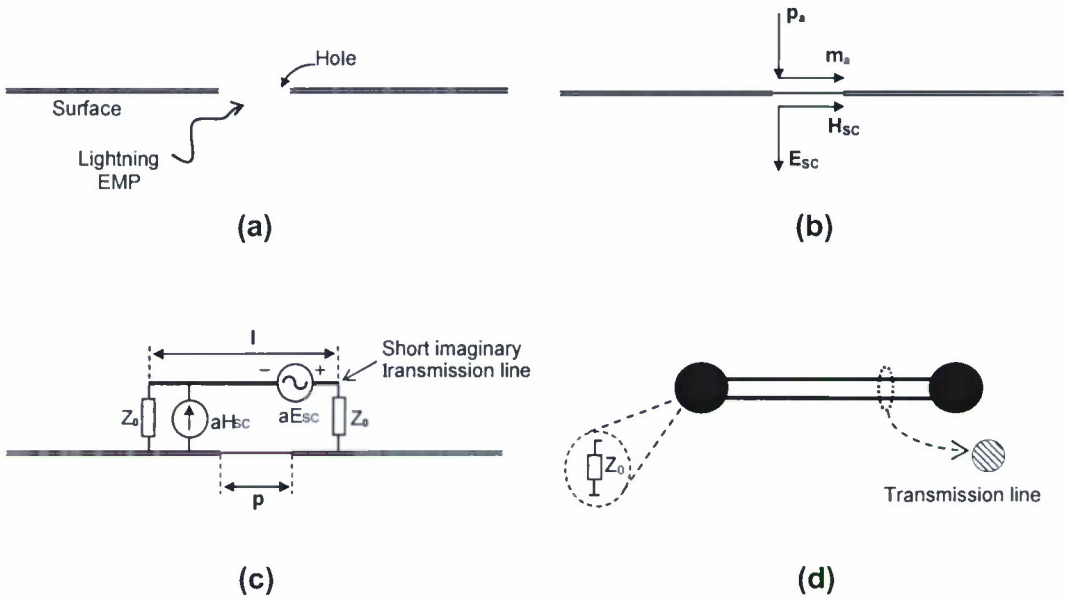

Fig. TF-1 Imaginary transmission line representing the field external couplings on the aircraft surface.

The system field penetration is described by the characteristics of the radiated fields caused by the short imaginary radiating dipole method. The radiated or incident electric field Einc and magnetic field Hinc, therefore, excite the transmission cable inducing the voltage and current

propagation. The relationship of the sources at the aperture and the fields at the interior cable through the transfer function can be written as

$$(Einc, Hinc) = TF(aEsc, aHsc).$$

Fig. TF-2 shows the variation in transfer function *TF* in with frequency and distance *R* under the lightning excitation. The transfer functions were determined through the relationship of aH_{sc} at the aperture and H_{inc} at 1, 5, 10, and 20 m from the aperture. For the cable excitation at a fixed distance from aperture, plots were also obtained ths completing the external-internal interaction processes and transfer function generation.

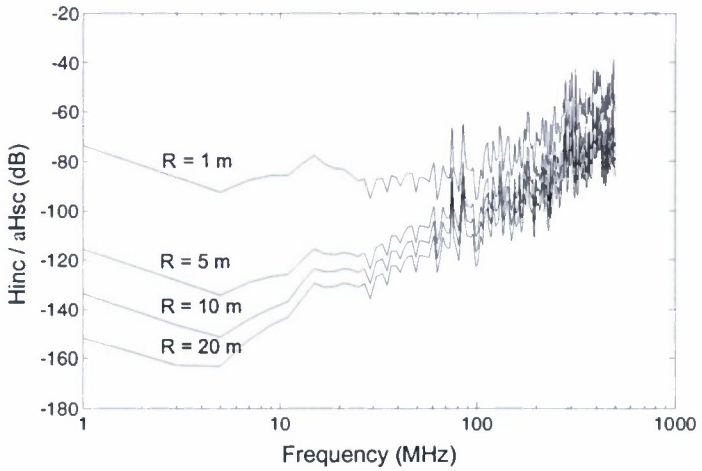

Fig. TF-2. Transfer function or the ratio of *Hinc* to *aHsc* in dB as functions of the distance *R* and frequency.

V. SUMMARY: INTERACTIONS WITH NETWORK CABLES

EMT-based simulations of the field-cable interactions in a network were implemented through the CRIPTE code by studying the communication between two PCs shown in Fig. NC-1(a), where the cable is connected to Ethernet cards in each computer. The Netgear 10/100 Mbps PCI model FA311 cards thus act as a junction for the CRIPTE code. Measured S-parameters will serve as the input to the junctions of the simulation network. Since the Ethernet card has only one physical port (although it may have two logical ports, one for sending another for receiving) the simulation target is to obtain the S_{11} parameters or the reflection coefficients. The data set of the measured S_{11} parameters is recorded from the network analyzer HP 85047A (300 kHz - 3 GHz) sweeping between 50 and 500 MHz. The measurement is carried out with and without power on the Ethernet card. The data is saved in the ASCII format. The file contains the data of amplitude and phase of S11 at 201 frequency points between 50 - 500 MHz. The ASCII file is then imported to the CRIPTE simulation using the ASCII-CRIPTE conversion feature. The output file from the conversion is in the S-matrix format, which is stored in the complex numbers at various frequencies. This file is read-in to the code at the appropriate junctions.
The plots of measured $|S_{11}|$ parameters of the network card in dB with and without the power are

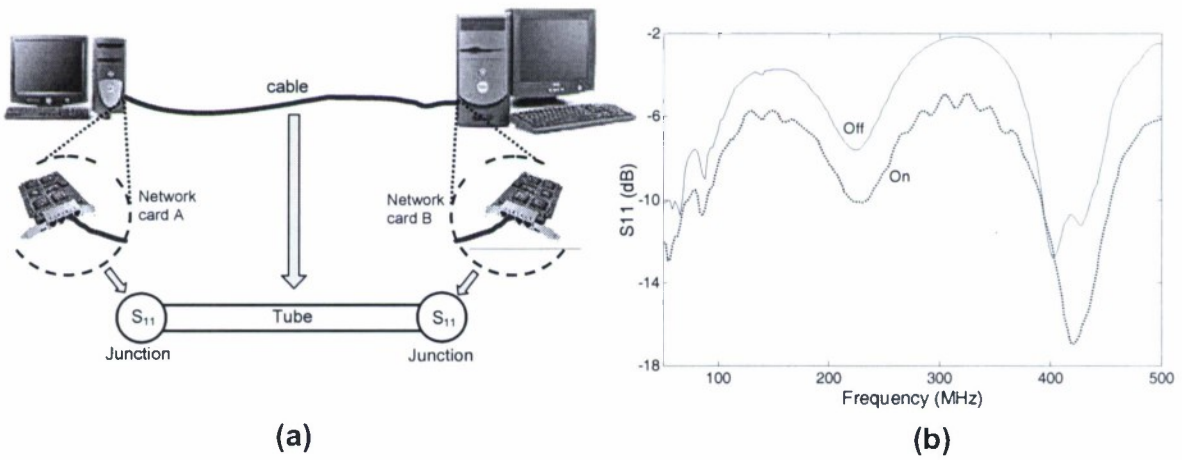

Fig. NC-1 (a) Configuration of communication network system with CRIPTE network representation. (b) Measured |S11| parameters (dB) on one port of the network card with and without the supplied power.

shown in Fig. NC-1(b) as labeled "on" and "off", respectively. The plots show that the least reflections occurred at 420 MHz and 400 Hz for the "on" and "off" cases, respectively. For the simulation study as long as the crosstalk is not our concern, instead of a basic communication multi-conductor cable (UTP CAT-5), the single wire cable with the same conductor dimension was used as to appropriately match with an only available data-sending port on the network card. Figs. NC-2 (a) and NC-2 (b), respectively, show the cable currents as a function of frequency along the cable length without and with the power to the network card. The results show that current due to the external sources are more pronounced at high frequencies and a probable cause for data fault or, communication breakdown. In addition, the simulation results also showed that the impact is more pronounced for the EMP than the direct-lightning strike.

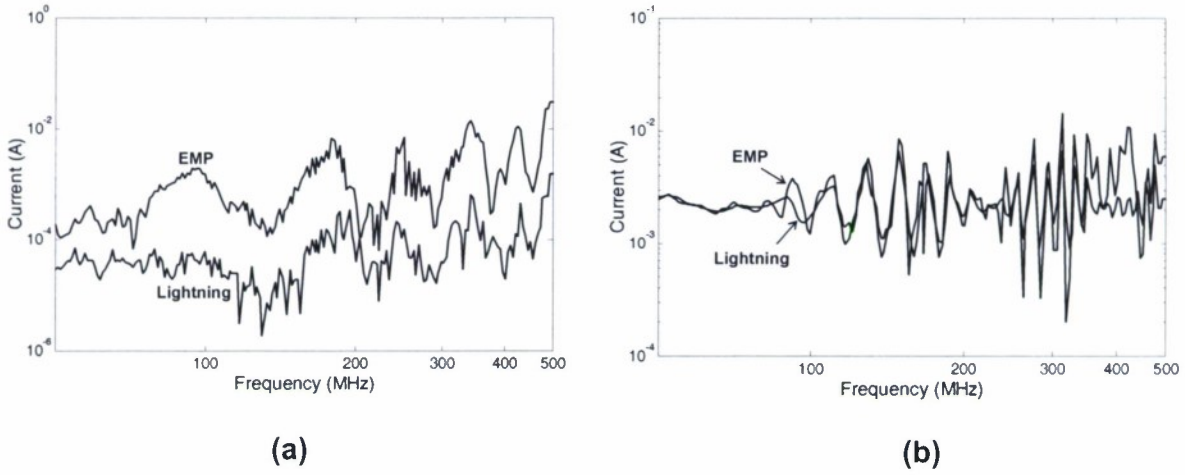

Fig. NC-2 (a) Current frequency responses on the cable when the network card is not powered under EMP (solid line) and lightning (dotted line) excitations. (b) Current frequency responses on the cable when the network card is powered under EMP (solid line) and lightning (dotted line) excitations.

Related Publications

A number of technical reports, papers and book article related to this novel application of CRIPTE code in the area of RF interactions were generated ([2006B1], [2005B1], [2005J2], [2005C6], [2005C7], [2004J1], [2004J2], [2004J3], [2004C1], [2004C2], [2004C3], [2004C4], [2004C5]).

VI. SUMMARY: INTEGRATED APERTURE INTERACTION EMT SIMULATIONS AND EXPERIMENTAL VALIDATION

For aperture field interactions a modified electromagnetic topological (EMT) simulation scheme was developed which was based on the scattering junction concept that provided a generic circuitry that looks into the for aperture interactions through a single EMT simulation step. Through this approach, it was possible to independently create individual junction in the circuitry that are based on the physics of interaction of the associated structure. This simulation process has the added advantage that it also takes into account the scattered field that is usually ignored in the original volume decomposition scheme.

An experiment to validate the results was also setup. Experiments were carried out for aperture-field interactions in a semi-anechoic chamber that involved a radiation source, an aperture of appropriate dimensions, and a cable at a certain distance from the aperture. Besides conventional Maxwell solver, simulations software also includes an EMT code in the frequency domain. The topological network is created is a multi-conductor transmission line network (MTLN) that can be formulated and solved by the BLT equation. So far, EMT has been used to simulate systems using measured scattering parameters, calculated scattering parameters, and cable assemblies with known geometry. To extend the utility of EMT, several researches and studies applied EMT to aperture interactions [1, 2]. The model has been verified by full-wave analysis methods such as Finite-Difference Time-Domain [3].

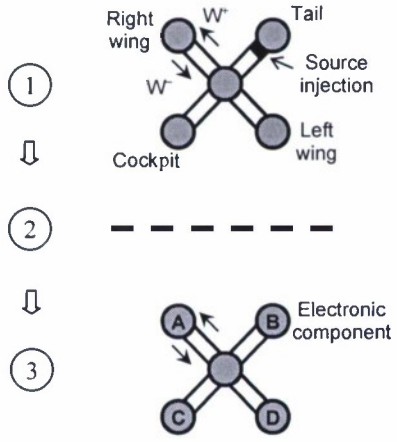

Figure SS-1 Original EMT computational scheme with upper-level and lower-level topological networks.

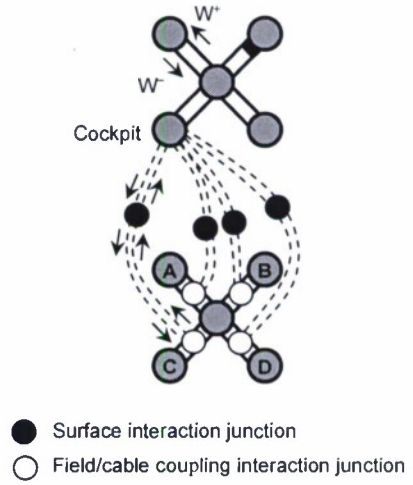

Figure SS-2 Proposed EMT computational scheme with interaction junctions between two networks..

However, the most logical way in the verification of the model is through experimental evidences. Based on original EMT scheme, the computation for entire network solutions needs to proceed through the three-step process, starting from the external volumes and ending at the internal electronic circuits, as can be seen in Fig. SS-1. By using the proposed

interaction scheme, the topological networks of two different levels in Fig. SS-1 can be merged as shown in Fig. SS-2. The interactions between two networks can be modeled using interaction junctions and linking tubes. This compact scheme reduces computation steps and preserves physics of interactions between two networks.

The experiments were conducted inside a semi-anechoic chamber of an Amplifier Research FS4010 test system as shown in Fig. SS-3.

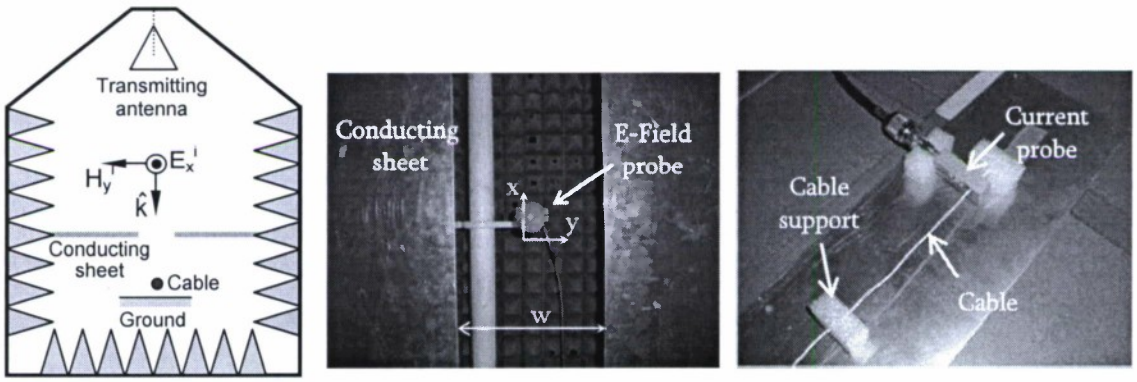

Figure SS-3 Experimental setup inside a semi-anechoic test chamber.

The range of interest for frequency measurement is set with a 10 MHz step increment from 100 MHz to 1.0 GHz. The solid line represents the frequency spectral contents of the measured incident electric field. The dashed line depicts the transmitted electric field. It is evident that the aperture behaves like a high-pass filter. The transmitted signals are attenuated at low frequencies while at high frequencies the transmitted signal follows the incident signal. The transfer function cutoff frequency associated with the aperture dimension is approximately 600 MHz. The fluctuation in the measured signal may be due to the effects of the hardware components and the non-perfect absorbers inside the semi-anechoic chamber. These observations will be giving an insight into the effect of the aperture on the cable current.

The induced currents on the cable from measurements through setups are shown in Figs. SS-4 and SS-5 respectively. The aperture effect can be activated by the junction. The cable resonances for both experiment and calculation cases are in accordance with the theoretical values, e.g., at 131 MHz for the first resonance. Even though the results from measurement agree relatively well with the output from EMT calculations, the discrepancy is probably due to mismatch of the probing cable and connectors that cause the 180° out of phase signal in opposition to the induced current at 500 MHz. As can be seen the presence of the aperture, the effect is similar where the resonances at lower frequencies are suppressed by the aperture. The frequency spectral amplitudes of first to fifth resonances from calculation are substantially decreased and this is also confirmed through measurements, providing the feasibility of the new electromagnetic topological scheme for a system level EMC problem.

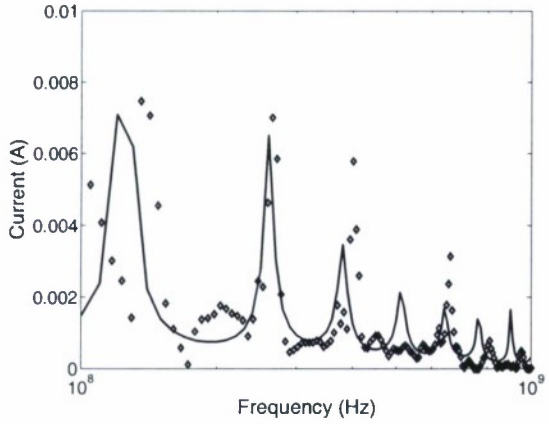

Figure SS-4 Induced cable currents from the measurement (diamonds) and from the EMT calculation using the topological network (solid line).

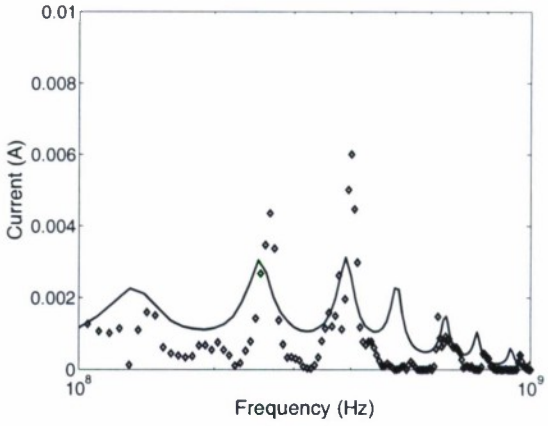

Figure SS-5 Induced cable currents from the measurement (diamonds) and from the EMT calculation using the topological network (solid line).

An advantage of this approach is the fact that new simulations with changes of substructures can be carried out without remodeling the entire system, as is required for conventional simulation methods.

VII. SUMMARY: MTLN-TLM ANALYSIS FOR APERTURE INTERACTIONS

In this study we proposed an alternate approach to simulate external EMP and aperture interactions, using a two step process. First there is an initial process of interaction that results in scattering fields at the aperture. These fields then propagate to the other side where further interactions may occur. The schematic of such an approach is shown in Fig. MTL-1 Here the EM wave interacts with a system primarily through the fields generated at the aperture in an infinite metallic plane, as shown. We concentrate primarily in generating the aperture fields and verify the results by comparing it with a FDTD code. In short, we propose a simpler and accurate methodology, which combines the EMT approach with the transmission line matrix (TLM) method to account for the coupling of an incident electromagnetic field with an aperture over an infinite metallic plane in a topological simulation setting. It does not require experimental field values for aperture radiation as was needed in our previous work. Finally, we also describe a method for applying compaction techniques that result in a more efficient computation without sacrificing accuracy.

EMT Compaction Solutions The TLM solution approach has been extensively used in many EM-related applications both in time and frequency domain. The time domain technique best suits simulating wave propagation in guided wave structures with arbitrary shapes and uses a band limited pulse excitation for studying frequency ranges. Thus for full impulse response, the simulations take a long time before steady state is reached, specifically for large network matrix. In this analysis we chose the frequency domain method because the topological network code works in the same domain.

For simulations without compactions, the matrix size required for each sub-network is 96 ($4 \times 1 \times 24$), i.e. 4-directional junction, 1-conductor wire, and 24 tubes. With compactions the original matrix reduces by half to $4 \times 3 \times 4 = 48$. We compute the matrix numerically just once and cascade this equivalent junction to others network arrays. The number of junctions required for the compacted network is 9 when the source junctions are not taken into account. Original network without compaction require 81 junctions.

The effects of the aperture width on the transmitted Gaussian pulse through the aperture are shown in Fig. MTL-2(b) where the solid lines are the frequency spectra from 50 MHz to 1.0 GHz, which are obtained by a Fourier transform on the FDTD generated E-field waveforms in the time-domain for the aperture widths d at 6 mm (case A), 12 mm (case B), 24 mm (case C), 36 mm (case D), respectively. Fig. MTL-2 (b) also shows the results based on topological simulations. The topological network used has nine sub-network components. The results show that energy coupled into the aperture decreases as the aperture dimension is decreased in accordance with the well known d^3 law whenever the wavelength is much smaller than the aperture width ($\lambda >> d$) [15]. The results also show that the amplitudes of the higher spectral components are less distorted as the aperture width increased. It is consistent with the analysis that the small aperture can be approximated using an undersized waveguide model with the very small thickness [16]. Therefore, in the frequency range smaller than the cutoff frequency, no waves can propagate through the aperture because of the inherent high-pass filtering properties. Incrementing the aperture size also results in the cutoff frequency to shift lower, allowing more penetration of the high frequency components.

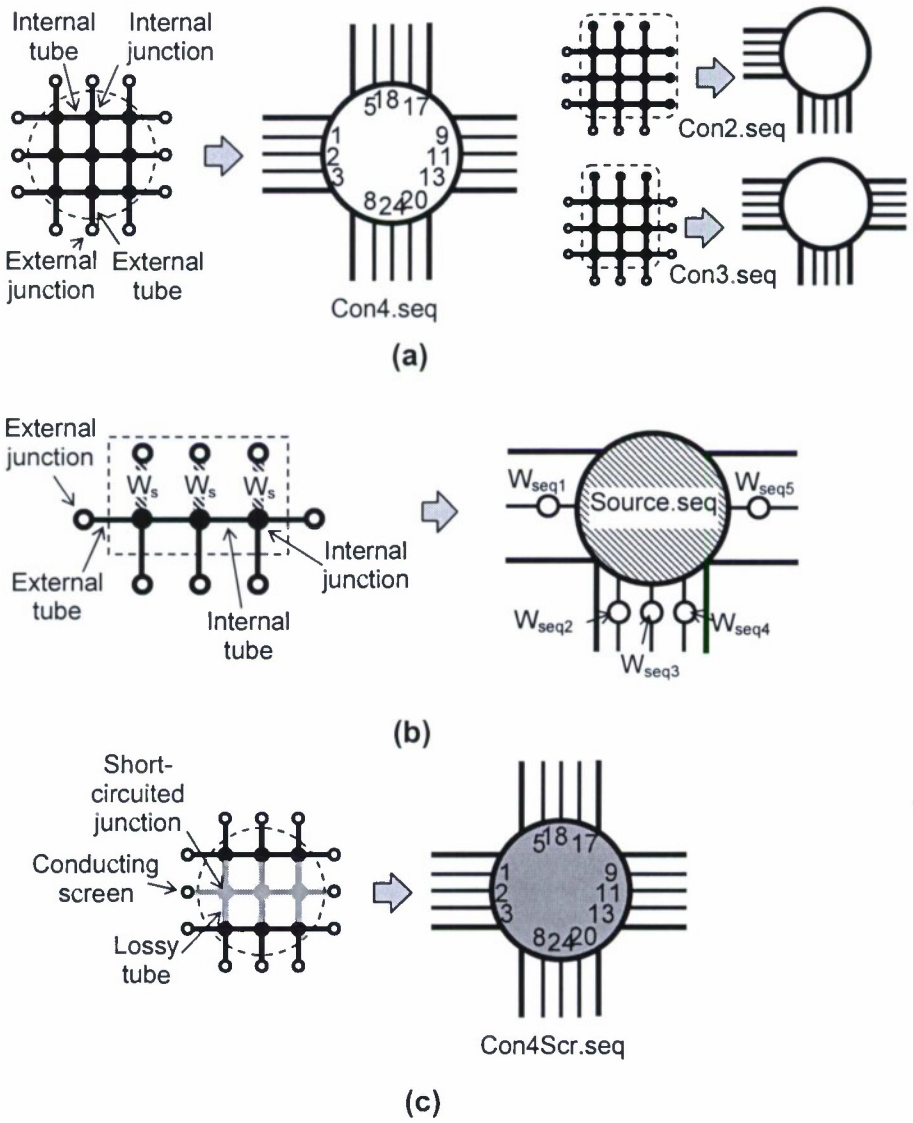

Fig. MTL-1 Compaction on the sub-network: (a) regular equivalent junctions, (b) equivalent junction with internal sources, and (c) equivalent junction with metallic conducting screen.

In Fig. MTL-2 (b), frequency spectra above the cutoff frequency of case D propagate through the aperture without significant distortion in amplitude while the lower frequency spectra experience frequency dependent attenuation. As the aperture size decreases from case D to case A, more components of the incident Gaussian pulse fall into below the cutoff frequency regions. The spectral components will experience stronger suppression and become flatter, increasing the

bandwidth. As a result, the fields transmitted through the aperture will be lower in amplitude caused by suppression and faster oscillation due to the larger relative weight of the high frequency spectral components than the incident pulse.

The calculation speed depends mainly on the resolution of the space step for time domain and the size of the compaction network for topological network domain. Simulations show that the ratio of the total elapsed time used for the FDTD and the topological calculations is 5.6, which is a huge advantage of using the compaction technique with the topological network. For FDTD code, a single calculation step is equal to a half distance of the cell dimension. One, therefore, requires 20000 time steps to achieve the result with corresponding first frequency of 10 MHz while the topological calculation needs 100 frequency steps from the fundamental to final frequency of 1000 MHz. The topological code has an advantage over the time domain code for this particular network size and it can be not true for more complicated arrangements. A validation of the time domain transmitted field for the 6mm case is shown in Fig MTL-2(a). Since TLM methods are applicable to low frequency, one can see slight discrepancy in the results as high frequency is approached. In addition, the delay of the wave from the EMT code reflects the property of the slow-wave propagation caused by the use of the shunt node-like configuration.

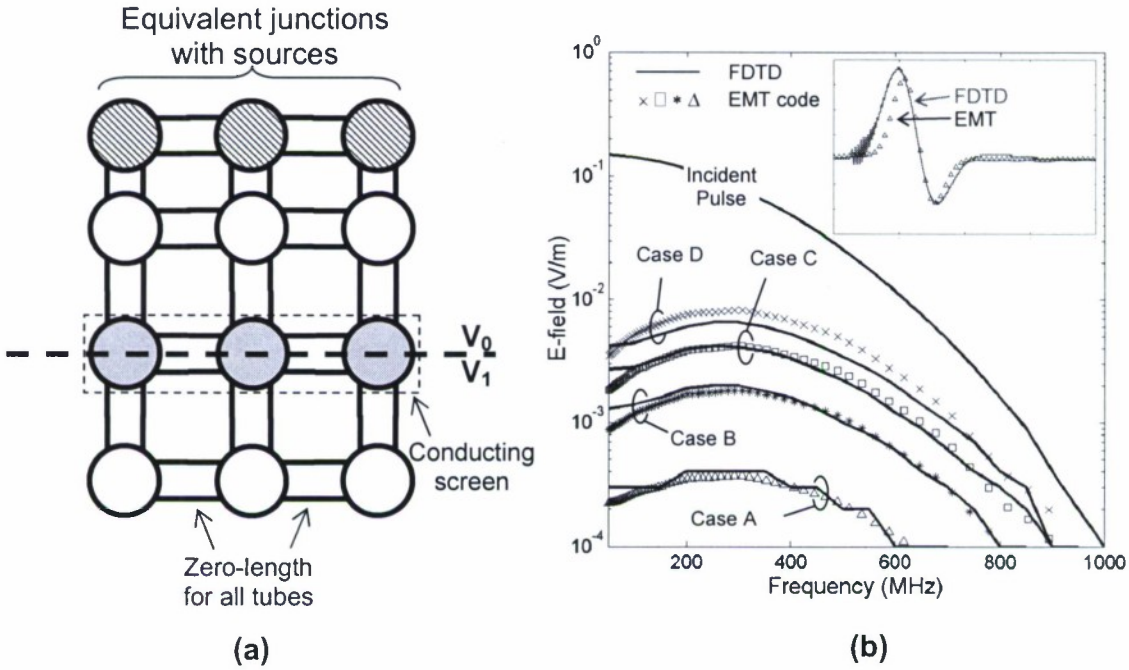

Fig. MTL-2 (a) Equivalent-junction network used in simulations. (b) Frequency spectral contents of the field transmitted through the conducting screen as a function of the aperture width (case A: 6 mm, case B: 12 mm, case C: 24 mm, and case D: 36 mm) from the FDTD calculations (solid lines) and the EMT-TLM calculations (various markers). Inset compares time-domain transmitted fields for the 6 mm case of both FDTD and EMT calculations.

Related Publications

Related works to this interaction study are reported in the paper [2006J3], and technical reports [2005C1], [2005C2], [2005C3], [2005C5].

VIII. SUMMARY: EMT ANALYSIS FOR CABLE CROSSTALKS

In this project an electromagnetic topology (EMT) simulation technique to study crosstalk induced in four pairs of UTP-CAT5 cables for frequency range up to a few hundred MHz was proposed. Simulation is based on a lumped-circuit transmission-line model similar to the configuration used in the work of Paul and McKnight [17, 18] where it consists of a single-wire generator, two-wire receptor circuit in a homogenous media. The wire separation and length are sufficiently small as to ensure a validity of a low-frequency model. The electromagnetic topology technique is a modular simulation method, specifically suited for electrical systems that are large and can be analyzed through volume decomposition [13]. The technique is to overcome some of the simulation problems associated with large network

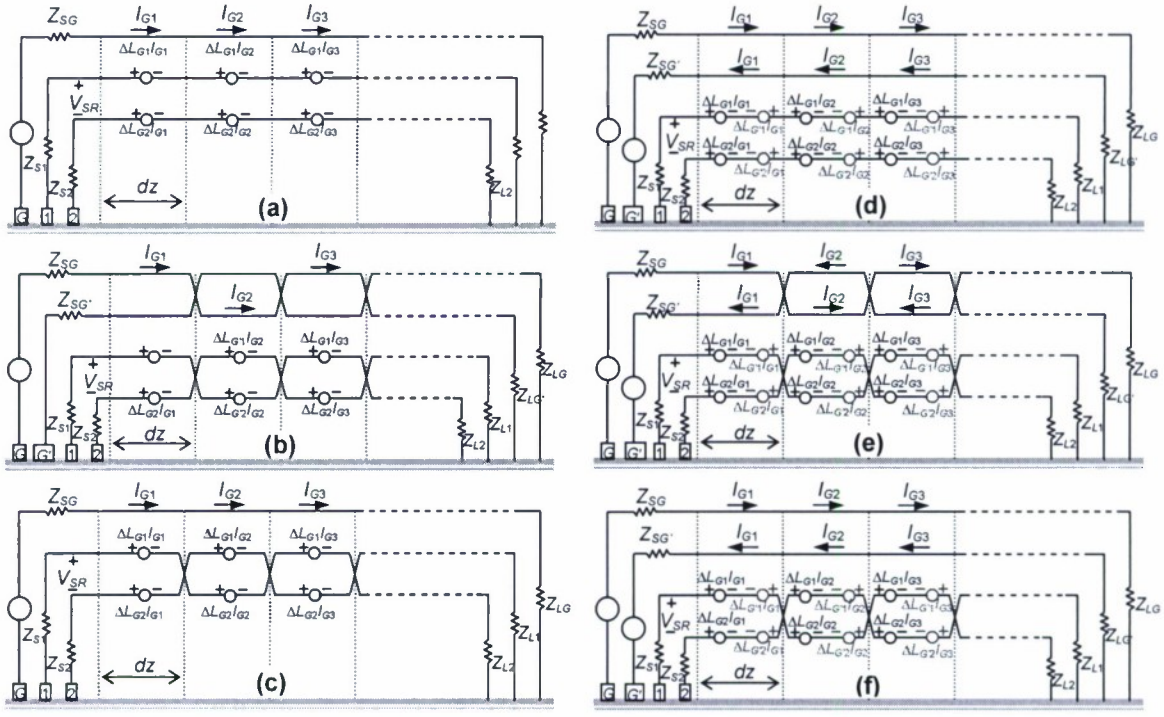

Fig. XT-1 Coupling models driven by single source of configurations (a) STS/STP, (b) TWP/TWP and (c) STS/TWP, and coupling models driven by differential source of configurations (d) STD/STP, (e) TWPD/TWP and (f) STD/TWP. $\Delta = jwL$.

systems. In an EMT simulation approach a very large network can be analyzed through volume decomposition.

In the simulation setup transmission-line model with various types of generator, receptor, and impedance arrangements are analyzed and compared effective crosstalk suppression on 100/1000Base-T networks. The outcome and advantage of such a simulation approach, besides the validation of topological simulation method, is a topological cross-talk suppressed circuit that can be integrated with a larger network for analysis.

Crosstalk Circuit Models Near End Crosstalk (NEXT) is a coupled interference signal between adjacent cables at the nearest end of the source. It does not depend on the generator and receptor cable length. The NEXT value (in decibels) is computed as the difference in amplitude between the test signal and the crosstalk signal, given by

$$NEXT = 20\log_{10}\left|\frac{V_{SR}}{V_{SG}}\right|,$$

where V_{SR} and V_{SG} are the voltages across the receptor and generator wires at the sending end, respectively. Higher negative values correspond to less crosstalk and better cable performance. By its nature, it will get worse as the frequency increases. In terms of interference the higher the frequency, the higher the noise coupling on the receptor or the smaller the electrical insulation between the interfering generator and the receptor. Fig. XT-1 shows the coupling scheme commonly used, while Fig. XT-1(b) shows the TWP/TWP model which is the most common configuration for the UTP-CAT5 cable where both generator and receptor circuits are formed by the twisted-pair wires (G-G' and 1-2). In this case, only single wire of the generator circuit is driven. The generator-receptor circuits in these figures can also be classified as straight-through differential-generator, straight-through receptor (STD/STP); twisted-pair differential-generator, twisted-pair receptor (TWPD/TWP), and straight-through differential-generator, twisted-pair receptor (STD/TWP).

Topological Network Approach The network under study is shown in Fig. XT-2(a) and includes a server hub, network computers, and UTP-CAT5 cable consisting of a bundle of eight conductor wires. The associated topological network is shown in Fig. XT-2(b), where it can be topologically decomposed into sub-volumes (junctions) interacting to each other through preferred paths (tubes). The junctions represent loads, branching of cables, or input impedance of electronic systems in the computer housings. The input and output waves are related to each other through a scattering matrix. The tubes between two junctions represent the homogenous sections of cable harness based on the multiconductor transmission line theory. The per-unit capacitance, inductance, and characteristic impedance matrices generated from the companion LAPLACE code are used to characterize the tube. The traveling waves at each end are related to each other through a propagation matrix, based on the multiconductor transmission line concept with scattering parameters at junctions and propagation parameters along tubes, the cable signals can be obtained through the BLT equations [20], given by where [I], [S], and [Γ] are the identity, network scattering, and propagation supermatrices, respectively. The terms [W(0)] and [Ws] are the outgoing and source wave supervectors, respectively. The general solution of the BLT equations is in frequency domain. The advantage of using the EMT technique is that all volumes will be treated independently from others.

$$\{[I]-[S][\Gamma]\}.[W(0)]=[S].[Ws], \qquad \text{(IIID-8)}$$

Cable Simulation Setup The per-unit values of cable parameters were obtained from an

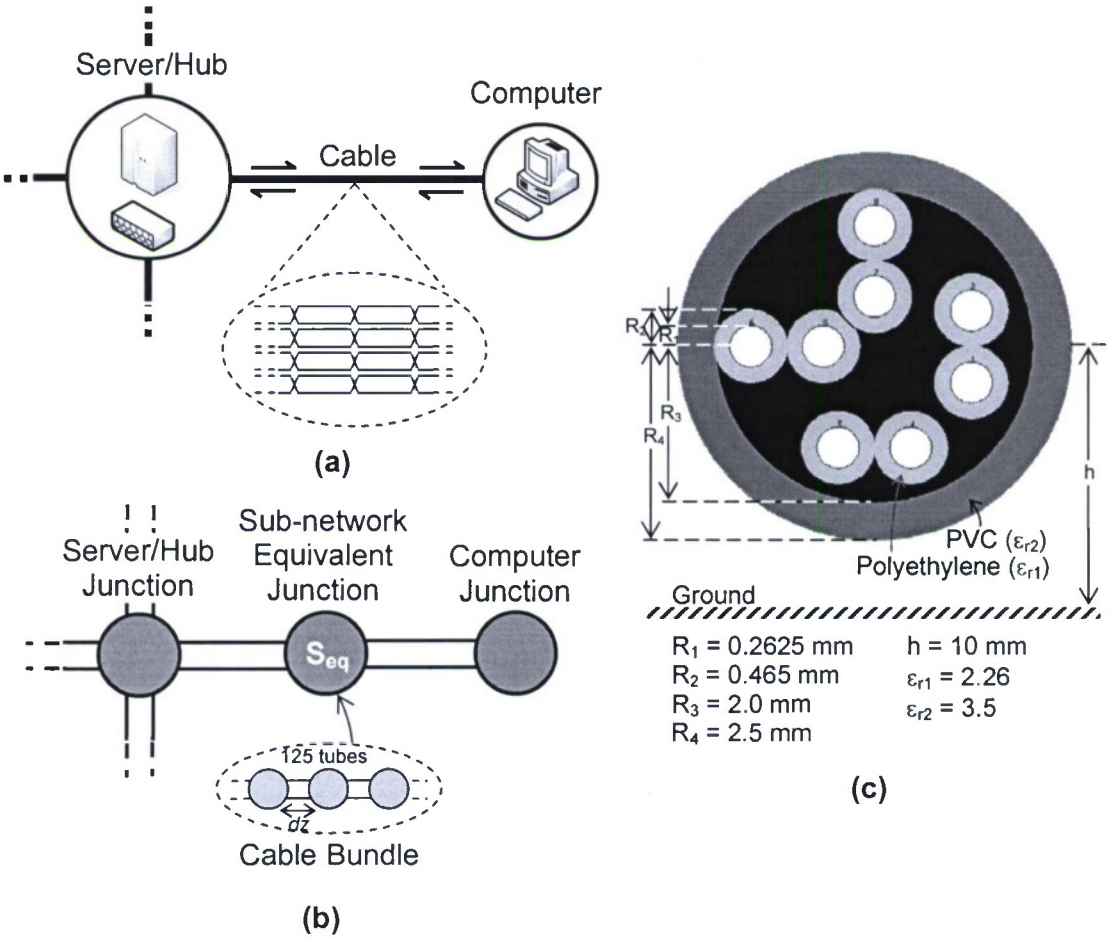

Fig. IIID-2 (a) Simple configuration of computer network and (b) associated topological network composed by junctions and tubes. (c) Cross-sectional view of the UTP-CAT5 cable consisting of four-pair conductors.

electrostatic calculation using the LAPLACE code based on the Method of Moments application, by meshing different sections of the multiconductor cable for capacitance and inductance matrices [21]. The cross-sectional configuration and details of the cable are shown in Fig. IIID-2(c), where it consists of eight dielectric-coated cylindrical conductors held together in four pairs and resided in the cable jacket. Each of eight conductors was also designed with the per unit length resistance of 100 mΩ/m. Each circular contour for the conductor and dielectric surface was defined with 10 expansion functions (1 + 9 cosine terms) and a triangular contour for the ground plane was defined with 30 linear distribution functions.

Sub-network Compaction In the simulations, the tube representing a 5-m long cable was decomposed into 125 tubes of homogenous sections with a length of 4 cm each. The junction characterizes the connection between two 4-cm tubes, which can be direct or twisted type corresponding to the circuit configurations shown in Fig. XTD-1. Since the entire length of cable comprises a large number of junctions and tubes with as many as eight conductor wires, direct calculation using the BLT equations is hardly cumbersome and time consuming. The matrix size required for such an exercise is large ($2 \times 8 \times 125 = 2000$), i.e. 2-directional junction, 8 conductor wires, and 125 tubes. If we were to assume that signals of interest are the waves traveling in and out the load junctions (concept of junction scattering), then it is possible to represent the whole cable network as a single equivalent junction, as shown in Fig. IIID-2(b). As a result, the original matrix reduces to $2 \times 8 \times 2 = 32$, decreasing computation time considerably. In addition, to realize a topological network with different terminal equipment, one needs only to change the boundary junctions without working out the entire topological network. With this setup, simulations were carried out to predict the near end crosstalk under various influencing parameters such as the value of the source and load impedances, the conductor pair location, and the cable driving source. The NEXT values were determined through (IIID-1) using crosstalk models related to (IIID-2) through (IIID-7) by applying a test signal to one cable pair and measuring the amplitude of the crosstalk signals received by the other cable pairs.

Crosstalk Reduction The computed results in Fig. XT-3 show the NEXT levels (1 kHz – 100 MHz) induced on the receptor pair 3-4, when the terminating impedances are 1 Ω and 1 kΩ. Fig. XT-3(a) shows results using the STS/STP, TWP/TWP, and STS/TWP models when the

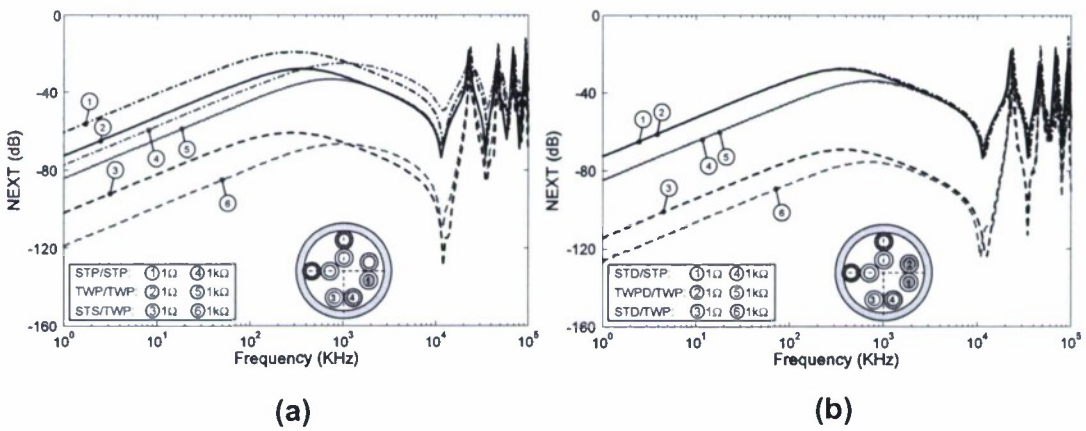

Fig. XT-3 NEXT levels across conductors 3 and 4 as a function of the source and load impedances (1 Ω and 1 kΩ) in frequency domain for coupling circuits driven by (a) + 0.5 V source on conductor 1 and (b) ± 0.5 V on conductors 1 and 2.

generator wire 1 is driven by a 0.5 V source. Figure IIID-3(a) shows linear curves at low frequencies and standing waves at high frequencies. One can see that the crosstalk induced

on the receptor wires is higher when the terminating impedance is 1Ω, e.g. at low frequencies, the value of curve 1 is approximately 16-dB higher than that of 15 kΩ (curve 4) for the STP/STP model. The reason is that, regardless of the capacitive coupling due to the balanced-load configuration, the inductive coupling is dependent on the generator current.

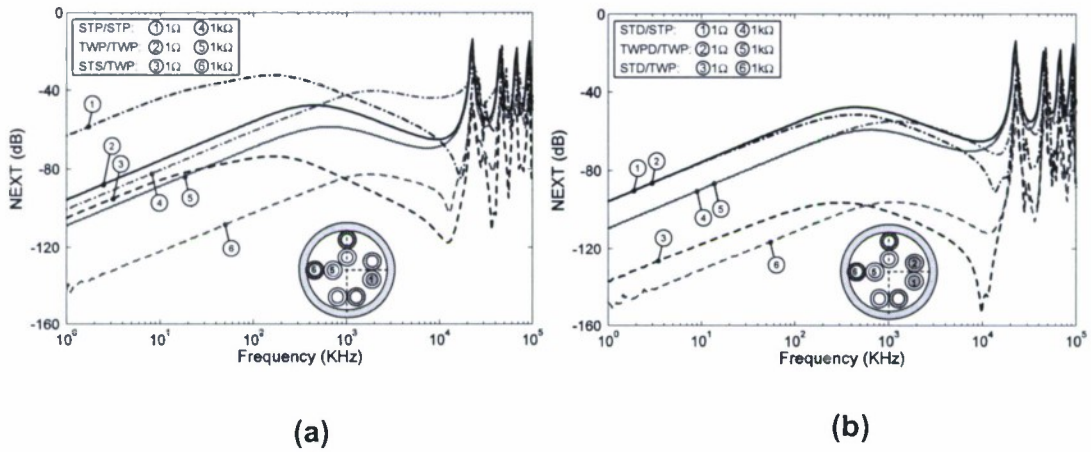

(a) (b)

Fig. XT -4 NEXT levels across conductors 5 and 6 as a function of the source and load impedances (1 Ω and 1 kΩ) in frequency domain for coupling circuits driven by (a) + 0.5 V source on conductor 1 and (b) ± 0.5 V on conductors 1 and 2.

The low impedances on the generator wire could result in a high value of current generated. Another observation is that the STS/TWP model provides the best in crosstalk reduction while the STS/STP model gives the worst performance. In other words, twisting either the generator or receptor pairs improves the effectiveness of crosstalk reduction, i.e. at 1 kHz and 1 Ω, the NEXT value of the STS/STP model is -60 dB while the STS/TWP's is approximately -100 dB. The different performances of crosstalk suppression can be directly explained by through theoretical expressions where the introduction of NMI term and SCG effect cause the reduction of the induced voltage. Simulations also showed that the multiconductor transmission line based simulation is less consistent when the length of the cable is considered electrically long or when curves enter the frequency of standing-wave region at above 1 MHz.

The next simulation examines the effects of using the balanced input technique. The results are compared with those obtained by driving a single wire generator. The computed NEXT results on the receptor pair 3-4 using the STD/STP, TWPD/TWP, and STD/TWP models are shown in Fig. XT-3(b) where the generator wires 1 and 2 are driven respectively by +0.5 V and -0.5 V source. Comparing results in Fig. XT-3(a), one can see the enhancement in crosstalk reduction. The enhanced performance of the NEXT suppression associated with curves 1, 3, 4, and 6 is due to the neutralizing mutual inductance created by the second driven generator wire. The improvement of crosstalk reduction is hardly noticeable for curves 3 and 4. Analyses of the results from the simulations are consistent with the analytical expression of all models. Clearly, twisting either the conductor pairs introduces the SCG-type

enhancement while balancing the input signal introduces the NMI term. The same can be said for the receptor pairs 5-6 and 7-8 as the associated computed results can be seen in Figs. XT-4 and XT-5 respectively for both types of driving signals.

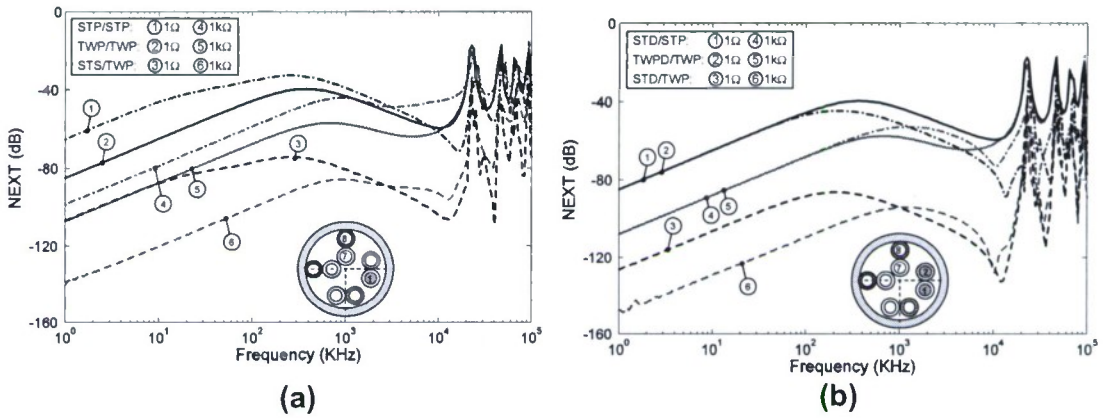

Fig. XT-5 NEXT levels across conductors 7 and 8 as a function of the source and load impedances (1 Ω and 1 kΩ) in frequency domain for coupling circuits driven by (a) + 0.5 V source on conductor 1 and (b) ± 0.5 V on conductors 1 and 2.

Since the crosstalk circuit model used in this work were analytically analyzed without considering the dielectric coating as well as the transmission line loss. As a result some discrepancy is expected between the analytical results and the EMT calculations, which account for the non-homogenous media and the current attenuation associated with the computer code-modeled UTP-CAT5 cable.

Related Publications

Related works to this interaction study are reported in the paper [2006J1] and technical report [2006C1].

IX. SUMMARY: EXPERIMENTAL VALIDATION OF EMT APERTURE INTERACTIONS SIMULATIONS

Electromagnetic field interactions and penetration through apertures have been studied for sometime [1-2] and this project focused in the same topic area but in the context of topological simulations using the electromagnetic topology (EMT) code and its experimental validation. The project helped us understand the details of coupling and interactions of the electromagnetic fields with electrical components, such as cables and printed-circuit boards, located inside an enclosure in the microscopics scale. EMT based simulations allows the results to be added in a modular fashion and ezch modeule can be a part of a larger system, such as an aircraft or a satellite. The EMT approach provides much faster turnaround times coupled with much reduced computer memory requirement, however, with acceptable accuracy for each module [3-5]. A particluar advantage of the EMT simulation approach over the usual Maxwell solver approach is the ability to handle apertures as one of the modules within electrical network system analysis to obtain the impact of apertures on the overall system response.

In our previous project, we proposed the EMT-based simulation techniques applicable for external-to-internal wave coupling through small apertures [6-7]. We based the simulation methodology, in part, by considering an imaginary transmission line that is used as an elemental source for aperture radiation. Then by using a transfer function, we came up with a total electromagnetic topology-based methodology that allows for direct coupling of an aperture to the rest of the electrical network system. In this report, we present the experimental result of the electromagnetic field penetrating through an aperture and compare it with the EMT-based simulation result for the same geometry by using assumptions and concepts presented in the earlier papers. We also compare the EMT simulation result with the finite-difference time-domain (FDTD) simulation result. The experimental result confirms the viability of the EMT simulation approach to predict the electromagnetic field interactions with apertures.

Both the FDTD and the EMT simulations are carried out on a Pentium XEON-processor Linux server. For the aperture interaction experiments, the free space test system, which is detailed in Section IV(C), is a state-of the-art system designed for RF radiated immunity and emissions testing for frequencies up to 1 GHz. We describe the experimental and simulation setups and present the aperture transfer functions obtained from the experimental and simulation validation process. The experimental setup used to study the interaction of the electromagnetic field with an aperture is seen in Fig. IVA-1. The test setup includes a free space test system, a semi-anechoic chamber, a log-periodic antenna, an isotropic field probe, and computer controller components. The process is controlled through a PC based LabVIEW interface. The 48×72 inch^2 metallic conducting plate placed inside the semi-anachoic chamber has a 6×10 inch^2 aperture in the center of the plate. The computer

controlled RF signal amplifier feeds the antenna, which is at a distance of 3 meters from the metallic plate to satisfy the far field condition at low frequencies.

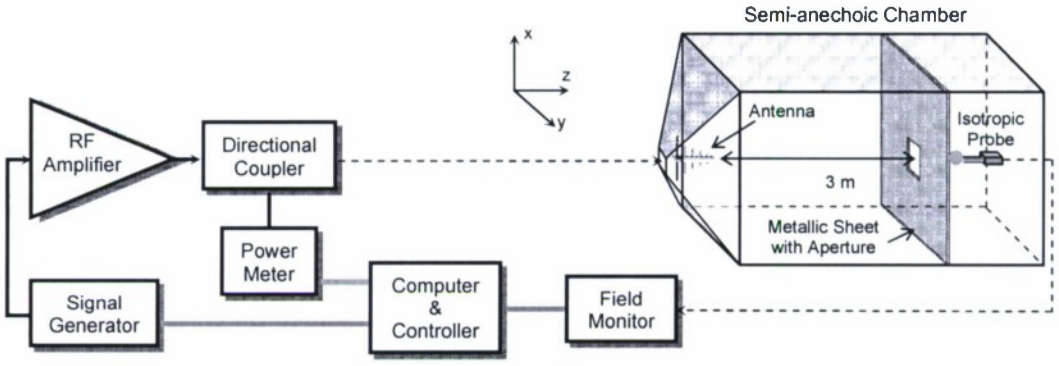

Fig. IVA-1 Experiment setup for an aperture interaction inside an anechoic chamber.

The range of interest for frequency measurement is set with a 10 MHz step increment from 100 to 1000 MHz. To account for leakage, reflection and diffraction of EM waves due to the size of the metallic plate and the chamber, the experimental data has been performed considering the following three-step process. First, the field monitor records the incident wave without the metallic plate inside the semi-anachoic chamber. Then, with the metallic plate in place, the transmitted field through leakage around the sheet is recorded by closing the aperture. In the last step the transmitted field through and around the plate is recorded by opening the aperture. The corresponding aperture transfer function is then calculated from recored electric fields as follows.

$$H_{ap}(\omega) = \frac{E_{trans,all}(\omega) - E_{trans,leak}(\omega)}{E_{inc}(\omega)} \qquad \text{(IVA-1)}$$

where $H_{ap}(\omega)$ is the aperture transfer function, $E_{inc}(\omega)$ is the incident E-field, $E_{trans,all}(\omega)$ and $E_{trans,leak}(\omega)$ are the transmitted E-fields with aperture opened and closed, respectively.

Fig. IVA-2 presents the aperture transfer functions associated with calculations of measured E-fields as discussed above and standard high-pass filter with the same cut-off frequency. As the figure shows, the aperture behaves as a high-pass filter with a cutoff frequency of approximately 590 MHz. The results are also consistent with aperture interactions previously studied with the aircraft under external excitation [8].

The overall simulation setup is shown in Fig. IVA-3, which describes the interaction mechanism associated with coupling between the front of the conducting plate and the aperture, i.e., Region I and the other side of the conducting plate, i.e., Region II. For EMT simulations, all the interactions have to be cast in terms of the external sources and the transmission lines [9]. The source would be the aperture itself, located on a conducting

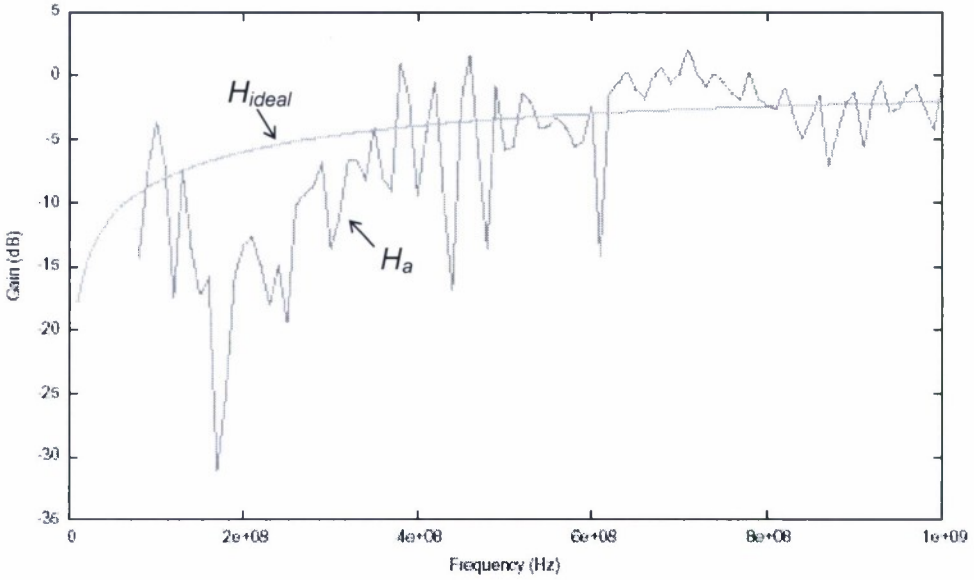

Fig. IVA-2 Measured aperture transfer function and standard high-pass filter.

surface of the metallic plate. It is represented equivalently as electric and magnetic dipole moments (p and m, respectively). In the low frequency limit, these dipole moments are determined by short-circuiting the aperture with perfect conductors [10]. Then the equivalent aperture dipole moments are given by

$$\mathbf{p} = 2\varepsilon_0 \vec{\alpha}_e \boldsymbol{E}_{sc} \tag{IVA-2}$$

$$\mathbf{m} = -2\vec{\alpha}_m \boldsymbol{H}_{sc} \tag{IVA-3}$$

where E_{sc} and H_{sc} are the short-circuit fields at the aperture, and the electric and magnetic polarizabilities (α_e and α_m) are determined both theoretically and experimentally [10]. The original and equivalent problems of aperture interactions are shown in Figs. IVA-3(a) and IVA-3(b), respectively. Once the equivalent dipole moment parameters are found, the next step is to calculate the field produced by both electric and magnetic dipole moments, represented, respectively, as Hertzian linear dipoles and loop antennas [11] seen in Fig. IVA-3(c). The length of the transmission line (d) is taken to be the same size as the actual width of the aperture.

The source value can be determined either from experiment, simulation or theory. We obtained the values of E_{sc} and H_{sc} through simulations using the FDTD method based on

Yee's algorithm in free space [12], where cell dimensions are much less than the minimum wavelength. The FDTD calculation is done for the computational volume of 240×240×6000 cm^3 with the uniform grid size of $\Delta x = \Delta y = \Delta z = 6$ cm. Once the grid size is defined, the next consideration is choosing the proper time step Δt to satisfy the Courant stability condition. The appropriate choice is $\Delta x/2c$, which gives 0.1 ns where c is the speed of light in free space. An incident 0.24-ns Gaussian pulse is applied as the x-polarized excitation.

The FDTD-simulated E_{sc} and H_{sc} are then applied to the external sources of the topological network in Region II. The short imaginary transmission line in the topological circuit, as a result of placing the Hertzian linear dipoles and loop antennas at the intersection of external and internal volumes, produces the radiated wave, which is used to come up an

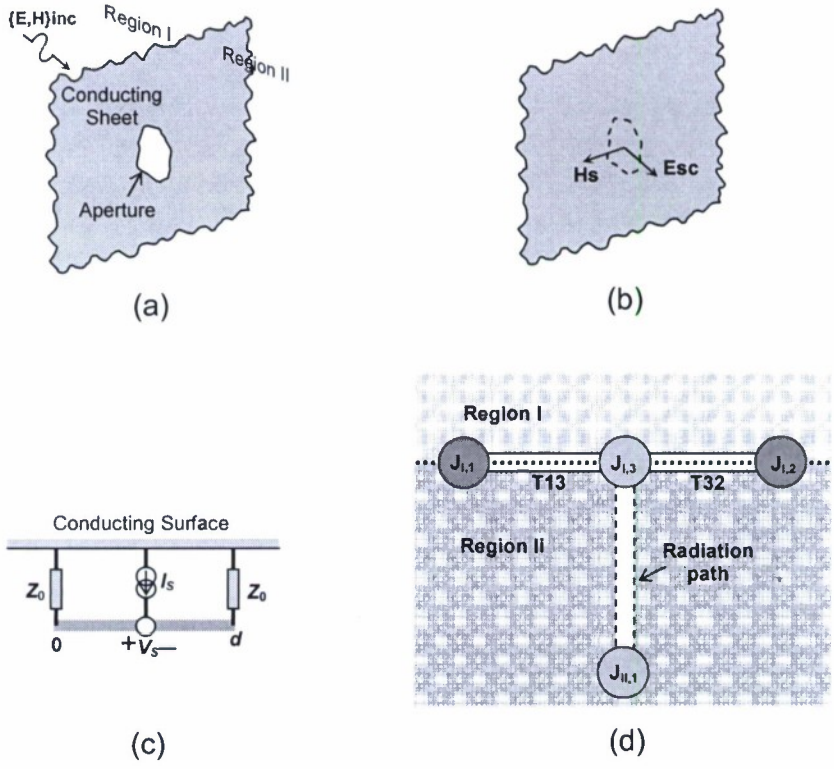

Fig. IVA-3 Aperture interaction diagram. (a) Original problem. (b) Equivalent problem. (c) Imaginary transmission line representing equivalent dipole moments. (d) Topological diagram for an aperture interaction.

external-internal transfer function. Assuming Δl represents the physical extent of the excitation zone, the driving voltage source for a Hertzian dipole antenna is given by

$$V_s = j\omega \frac{\mathbf{p}}{d} Z_0 \Delta l \qquad \text{(IVA-4)}$$

where d is a dipole length, Z_0 is antenna characteristic impedance, which is 377 Ω, and p is

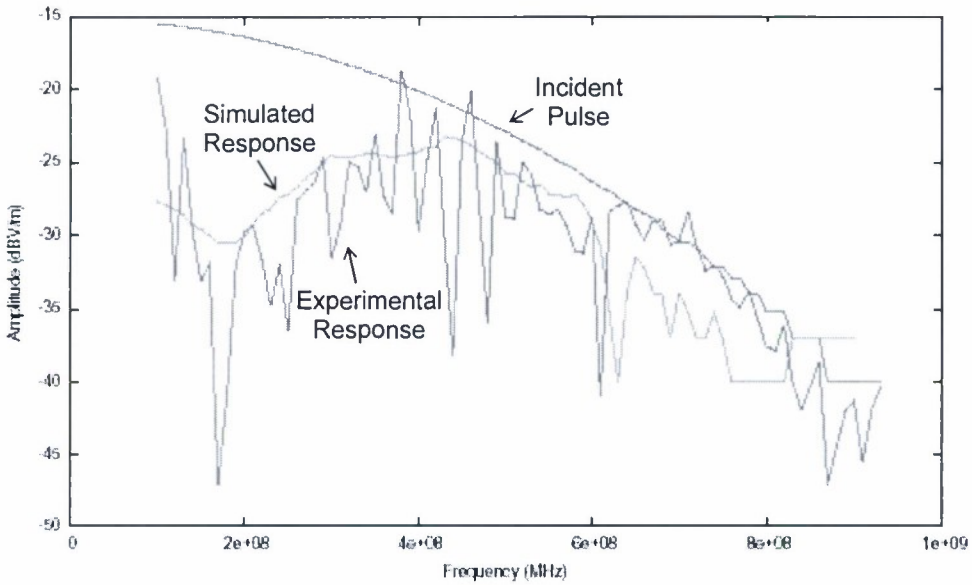

Fig. IVA-4 Incident pulse, topological simulated response, and experimental response.

given in (IVA-2). Similarly for a Hertzian loop, the driving current source is given by

$$I_s = \frac{\mathbf{m}}{S}\Delta l \approx \frac{\mathbf{m}}{d^2}\Delta l \qquad \text{(IVA-5)}$$

where S is a loop area and can be approximated by d^2. The parameter **m** is given in (IVA-3).

Fig. IVA-3(d) is the topological network representing the diagram found in Fig. IVA-3(c). A tube connecting two junctions represents the transmission line. Junctions $J_{I,1}$ and $J_{I,2}$ represent the termination impedances Z_0. Tubes T_{I3} and T_{32} connecting these two junctions represent the transmission line. The voltage and current sources are applied at junction $J_{I,3}$ as the external sources of the topological network in Region II. The relationship of junctions $J_{I,3}$ and $J_{II,1}$ is proportional to the radiated wave though aperture (broken-line tube). Junction $J_{II,1}$ is the location connecting a number of electronic circuits and equipments in Region II. This approach greatly simplifies the EMT simulation set up for implementation in the EMT method; however it is very cumbersome and difficult in the FDTD method. A comparison of the measured and topological simulations is shown in Fig. IVA-4. The blue and green lines represent the measured and simulated results of the transmitted E-fields, respectively. The frequency components below the cutoff frequency are suppressed while less distortion is observed for components above the cut-off frequency. This comparison, based on earlier assumptiond for EMT-based aperture interactions, shows a good agreement between experimental and simulated results.

Accomplishments: Two conference presentations (AMEREM, DEPS) and one draft sent for IEEE journal publication.

X. SUMMARY: EMT BASED TECHNIQUE TO MINIMIZE CROSSTALKS IN UNSHIELDED TWISTED-PAIR CABLES TOPOLOGY TECHNIQUES

In this project crosstalk reduction is analyzed for a reconfigured category-five cable network using electromagnetic topology-based simulation. The reconfigured network results in a marked reduction in inductive near-end crosstalk for the unshielded twisted-pair cable network. Analyses show that half-loop shifting of the generator-pair wires placed next to the receptor is the most effective way to control the near-end crosstalk level. This is primarily due to additional coupling sources induced on receptor wires that effectively deactivate the original cross coupling effect. The analysis also reveals the usefulness of electromagnetic topology-based simulations. The technique applied in this paper is applicable for any large network systems. A sub-network compaction scheme is critical in creating the equivalent junctions that provide a significant reduction in total computational time and total computer memory requirement for analyzing large network systems. For a 5.28-m long cable we have considered in this paper, the results are valid up to 10 MHz.

Crosstalk management has been the biggest challenge in optimizing the performance of cable networks, consisting of unshielded twisted-pair (UTP) wires. Emission, interference and crosstalk are important parameters that determine the overall cable network performance. To ensure an efficient cable network performance, these parameters must be dealt with by performing a detailed electromagnetic interference (EMI) analysis. For the cable network system consisting of UTP wires, one possible scheme to reduce the interference is introduction of the radiated signals that are equal but opposite of the unwanted signal values on all the wires inside a cable. This results in the subsequent cancellation of unwanted signals, making the network system an inefficient radiator. Crosstalk of twisted pair wires inside a cable is defined as the undesirable signal transmission from one wire pair to all other wire pairs. Similar to electrical noise coming from outside sources, crosstalk results in severe degradation of overall network performance.

A number of studies have been carried out in the past for the EMI analysis involving crosstalk in twisted-pair wires inside various cable types [13-18]. There are three basic models used particularly in these analyses: the bifilar helical-type model, the chain-parameter model, and the two-wire transmission-line model. Maki *et al.* [14] investigated the crosstalk margin level of a UTP-CAT5 cable in the frequency range up to 100 MHz for a 10/100 Base-T home network [19]. All such analyses showed the resulting crosstalk depended to a large extent on the values of line-termination or load impedances.

We present an alternative simulation approach used to investigate crosstalk reduction. We utilize the electromagnetic topology (EMT)-based simulation technique to study the crosstalk induced on twisted pair wires of UTP-CAT5 cables for a frequency up to a few hundred MHz. Simulation is based on a lumped-circuit transmission-line model similar to the configuration used in the work by Paul and McKnight [15-16] where they investigated a single-wire generator/two-wire receptor circuit in homogenous media. Wire separation and

length are sufficiently small to ensure the validity of a low-frequency model. In this paper, we propose a concept of electromagnetic topology simulation to account for the crosstalk caused by signals propagating through connecting cables using the EMT-based CRIPTE code [21]. In our previous crosstalk studies, we showed that crosstalk reduction is possible by twisting either the generator or receptor pairs [22]. However, the type of the cable specified in the study is not commercially available. A modification of the off-the-shelf cable is proposed in this paper to achieve the same objective without having to incur huge additional investment costs for reduced crosstalk cable designs.

In the EMT-based simulation setup, we incorporate the multi-conductor, transmission-line model with various types of generator, receptor, and impedance arrangements to analyze and compare the effective crosstalk suppression on 10/100 Base-T networks. The advantage of such a simulation approach, besides the validation of topological simulation method, is the ability to isolate topological circuit elements of a large network for crosstalk suppression analysis that can be integrated later into a larger network for the overall network response evaluation. Detailed approach to the proposed crosstalk circuits for twisted-pair cables, the simulation setup, and the results and discussion are as follows.

Near-end crosstalk (NEXT) is a coupled interference signal between adjacent cables at the nearest end of the source and computed as the difference in amplitude between the test signal and the crosstalk signal, given by (in dB)

$$NEXT = 20\log_{10}\left|\frac{V_{SR}}{V_{SG}}\right|,$$

where V_{SR} and V_{SG} are the voltages across the receptor and generator wires at the sending end, respectively. Larger negative values correspond to better cable performance.

Fig. IVB-1 shows the coupling schematic of a four-wire cable system that has been adapted for the analysis of the configuration of a four-pair cable system shown in Fig. IVB-2. Circuits shown in Figs. IVB-1(a) and IVB-1(b) are schematic representations of a two-wire generator, two-wire receptor circuits driven by single source (V_G) and differential sources (V_G and V_G), respectively. Unlike TWP/TWP and TWPD/TWP circuit configurations studied in [23], the generator-wire pair is shifted to the left by a distance of half-loop length ($dz/2$). The circuit in Fig. IVB-1(a) is a half-loop shifted twisted-pair single-generator/twisted-pair receptor (HLS-TWP/TWP). Based on the low-frequency approximation, we consider the case where voltages and currents of each section are approximately the same [21]. It is important to note that all analytical circuits to be discussed are modeled with balanced loads. As a result, the contribution to the crosstalk on the receptor pair is mainly coming from inductive coupling [16]. The differential voltage between receptor wires at the sending end (V_{SR}) can now be expressed as

$$V_{SR} = \left[\frac{Z_{SR}}{Z_{SR}+Z_{LR}}\right] j\omega L_{G1} dz I_{G1} + \tfrac{1}{2} j\omega L_{G'1} dz I_{G2} + \tfrac{1}{2} j\omega L_{G'2} dz I_{G2} + \ldots$$

$$\ldots - \tfrac{1}{2} j\omega L_{G'1} dz I_{G2} - \tfrac{1}{2} j\omega L_{G'2} dz I_{G2} - j\omega L_{G2} dz I_{G1}$$

$$V_{SR} = \left[\frac{Z_{SR}}{Z_{SR}+Z_{LR}}\right] j\omega dz (L_{G1} - L_{G2}) \cdot I_{G1}, \qquad)$$

where Z_{SR} and Z_{LR} are source and load impedances, respectively, L_{G1} and L_{G2} are mutual inductances between the generator wire G and receptor wires 1 and 2, respectively, $L_{G'1}$ and $L_{G'2}$ are mutual inductances between the generator wire G' and receptor wires 1 and 2, respectively, and I_{G1} is the generator current of the first twisted segment. The induced sources due to the original twisted-pair configuration without shifting are labeled with A_n, where n stands for the nth loop on the receptor wires [22]. With the proposed configuration, the identical coupling voltage sources are inductively induced on the left side of the twisted junction on the receptor wires labeled as B_{n-1}. One can see the source cancellation caused by identical sources B_n and A_{n+1} with opposite polarity. Consequently, I_{G1} is the only contributor to the expression for V_{SR} in Eq. (above) for any number of twisted loops. Comparisons of the Eq. with the previous equations in [23]) show that this Eq. resulted in the absolute minimum NEXT value, i.e., maximum crosstalk reduction.

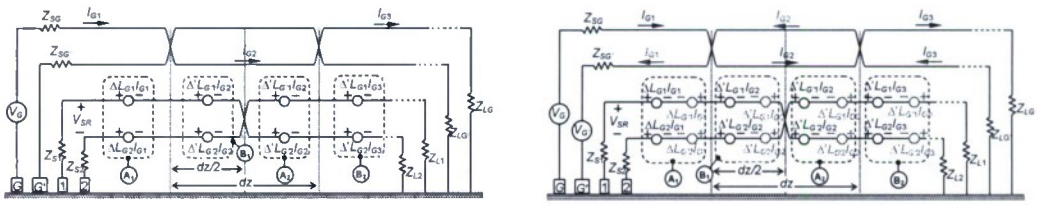

(a) (b)

Fig. IVB-1 Coupling models of a four-wire cable system with a generator-wire pair shifted to the left by a distance of half-loop length: (a) HLS-TWP/TWP driven by single source, and (b) HLS-TWPD/TWP driven by differential source. Note: $\Delta = jwL$ and $\Delta' = \frac{1}{2}jwL$.

For a half-loop shifted, twisted-pair differential-generator/twisted-pair receptor (HLS-TWPD/TWP) circuit shown in Fig. IVB-1(b), both generator wires are driven by differential input sources. The use of differential signaling technique, also known as balanced input, has distinct advantages by providing immunity to noise pickup and crosstalk between channels. The receptor differential voltage is expressed as

$$V_{SR} = \left[\frac{Z_{SR}}{Z_{SR}+Z_{LR}}\right] j\omega L_{G1} dz I_{G1} - j\omega L_{G'1} dz I_{G1} + \tfrac{1}{2} j\omega L_{G'1} dz I_{G2} - \tfrac{1}{2} j\omega L_{G1} dz I_{G2}$$

$$+ \tfrac{1}{2} j\omega L_{G'2} dz I_{G2} - \tfrac{1}{2} j\omega L_{G2} dz I_{G2} + \ldots + \tfrac{1}{2} j\omega L_{G1} dz I_{G2} - \tfrac{1}{2} j\omega L_{G'1} dz I_{G2}$$

$$+ \tfrac{1}{2} j\omega L_{G2} dz I_{G2} - \tfrac{1}{2} j\omega L_{G'2} dz I_{G2} + j\omega L_{G'2} dz I_{G1} - j\omega L_{G2} dz I_{G1}$$

$$V_{SR} = \left[\frac{Z_{SR}}{Z_{SR} + Z_{LR}}\right] j\omega dz\{(L_{G1} - L_{G2}) - (L_{G'1} - L_{G'2})\} \cdot I_{G1}. \qquad \text{(IVB-3)}$$

Similar to the HLS-TWP/TWP model, the source cancellation is the main reason for better crosstalk reduction. Also, as the case with the expression for V_{SR} in Eq. (IVB-2), I_{G1} is the only contributor for V_{SR} in Eq. (IVB-3) for any number of twisted loops. Furthermore, the equivalence of (L_{G1}-L_{G2}) and ($L_{G'1}$-L_{G2}) could cause V_{SR} to be even more effective in crosstalk reduction.

For an eight-wire cable system, a schematic diagram is shown in Fig. IVB-2. The generator and receptor wires are labeled as #1-2 and #3 through 8, respectively. The generator pair is shifted to the left by the distance of the half-loop length. Each junction

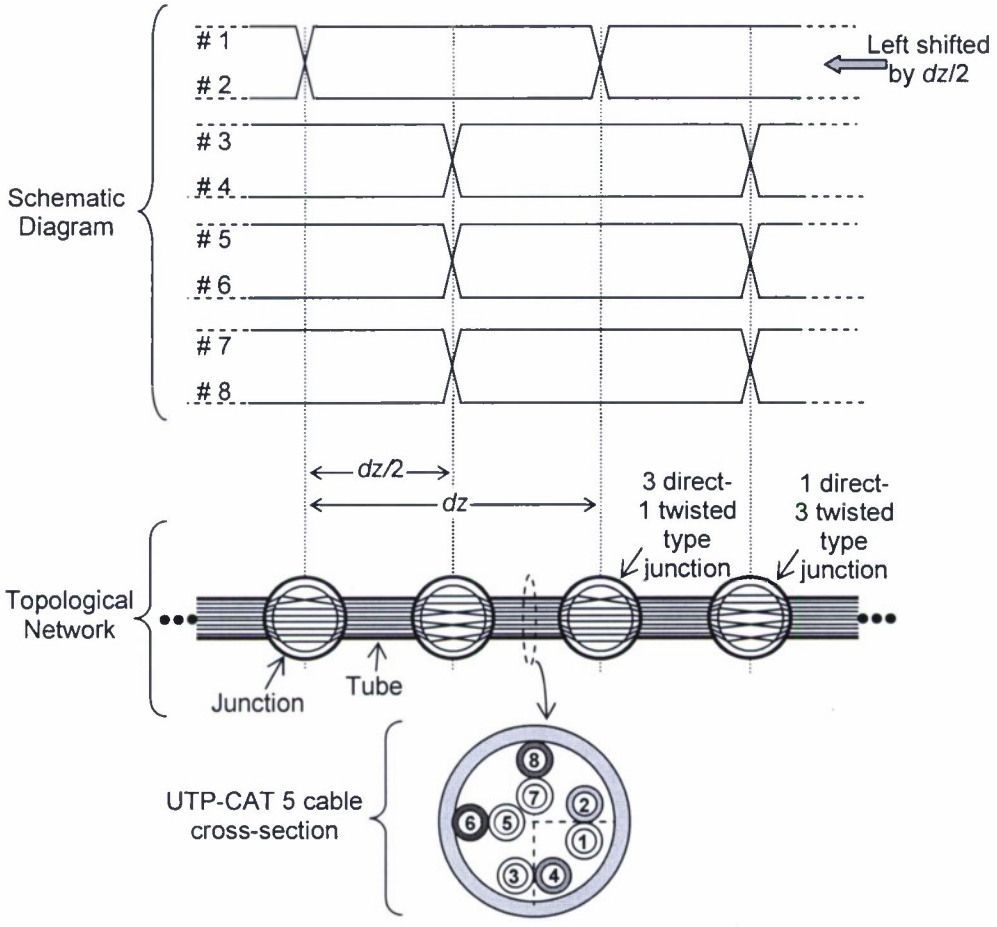

Fig. IVB-2 Representations of a four-pair cable system with the proposed half-loop shifting method, the associated junction-tube topological network, and the actual UTP-CAT5 cable cross-section.

characterizes a cable connection for all the direct and twisted type generator-wire and receptor-wire pairs. Each tube represents each section of the actual UTP-CAT5 cable with associated cross-section geometry shown in Fig. IVB-2. Traveling waves at each junction are related to each other through a propagation matrix. Using the BLT equation [20] with scattering parameters at junctions and propagation parameters along tubes, the cable signals, which are functions of traveling waves, can be expressed as

$$\{[I]-[S][\Gamma]\}.[W(0)]=[S].[Ws], \qquad \text{(IVB-4)}$$

where [I], [S], and [Γ] are the identity, network scattering, and propagation supermatrices, respectively. The terms [W(0)] and [Ws] are the outgoing and source traveling wave supervectors, respectively.

The cross-sectional area of the cable is shown in Fig. IVB-2. It consists of eight dielectric-coated cylindrical conducting wires held together as four sets of two wire pairs inside the cable jacket. Details are discussed in [22]. The companion LAPLACE code, which is based on the Method of Moments, is used to determine capacitance and inductance matrices from the cable cross-sectional dimension. In our EMT-based simulation, a 5.28-m long cable is divided into 264 tubes of homogenous sections with a length of 2 cm each. The junction characterizes the connection between two 2-cm tubes, either 1 direct-3 twisted or 3 direct-1 twisted type, for the configurations shown in Fig. IVB-2. Since the entire length of cable turned out to be a large number of junctions and tubes by considering as many as eight conductor wires, the direct calculation of the BLT equations is very time consuming. However, it is possible to break the spread network into many sub-networks, and then treat each sub-network separately using the diakoptics technique, which is suitable for the

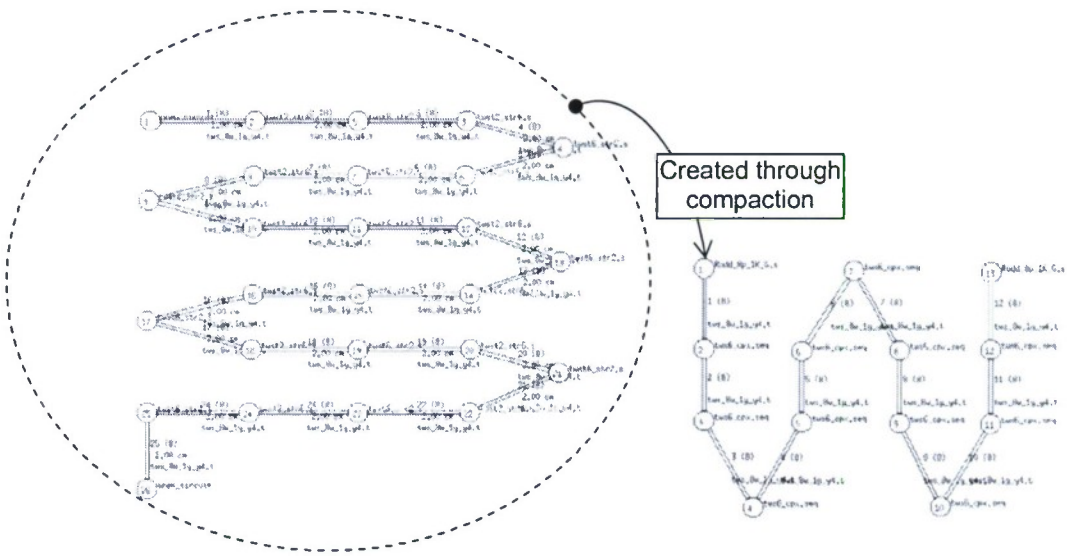

Fig. IVB-3 Simulation setup for HLS-TWP/TWP and HLS-TWP/TWPD circuit configurations where each subnetwork is created from 25 tubes representing an equivalent junction of a 48-cm long cable. The topological network of the final integration of 12 tubes, 11 equivalent junctions, and two impedance junctions represents a 5.28-m long UTP CAT5 cable.

repeated analysis of a large number of sub-networks with a slight difference seen in elements of all the sub-networks [23].

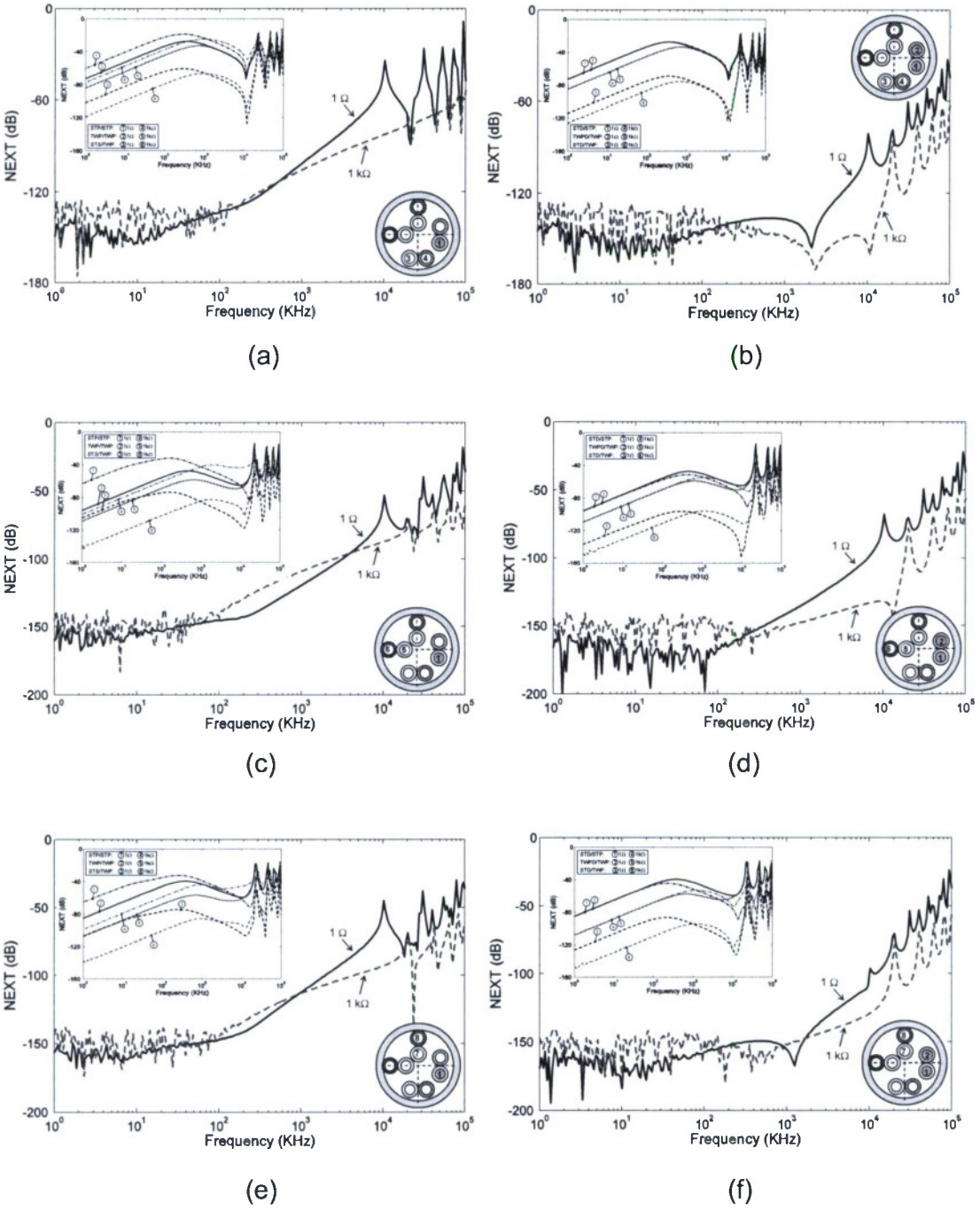

Fig. IVB-4 NEXT levels across Conductors 3-4 ((a) and (b)), Conductors 5-6 ((c) and (d)), and Conductors 7-8 ((e) and (f)) as functions of the source and load impedances (1 Ω and 1 kΩ) in the frequency domain for coupling circuits driven by a +0.5 V source on conductor 1 and ±0.5 V sources on Conductors 1 and 2. The plots shown in the inset are the results using different crosstalk models from the previous study [22].

Such a compaction technique allows for much faster calculations by creating the equivalent junctions. Consequently, there is no need to re-compute all sub-network contributions to a large network at various frequencies. For our case, each sub-network is created from 25 tubes representing a section of 48-cm long cable, as shown at the left-hand side of Fig. IVB-3. An equivalent junction (tws6_cpx.seq) is then created through compaction. The right-hand side of Fig. IVB-3 shows the topological network of the final integration of 12 tubes, 11 equivalent junctions, and 2 impedance junctions, corresponding to a 5.28-m long UTP-CAT5 cable for the HLS-TWP/TWP and HLS-TWP/TWPD circuit configurations found in Fig. IVB-1.

Computed near-end crosstalk levels (1 kHz – 100 MHz), induced on the receptor-wire pair 3-4, are shown in Figs. IVB-4(a) and IVB-4(b). Plots shown in Fig. IVB-4(a) are the results of using the HLS-TWP/TWP model when the Generator Wire 1 is driven by a +0.5 V source with the load impedances of 1 Ω and 1 kΩ, respectively. The figure also shows the cable cross-sectional geometry with the active wires labeled as 1-2 for the generating wires and 3-4 for the receptor wires. Fig. IVB-4(a) shows significant suppression in crosstalk levels at low frequencies and elevated levels of crosstalk during a standing wave region at high frequencies. One can also see the crosstalk induced on the receptor wires is higher at high frequencies when the load impedance is 1 Ω as compared to the load impedance of 1 kΩ. The reason is that, regardless of the capacitive coupling, the inductive coupling depends on the generator current. Low impedances on the generator wire results in a higher value of the generated current. The inset plots are the crosstalk levels (1 kHz – 100 MHz) of different models from previous study (STP/STP, TWP/TWP, and STS/TWP models in [22]). Compared to the results obtained by using the proposed model with those shown in the inset, the HLS-TWP/TWP model gives the best crosstalk reduction. The technique of shifting the generator loops improves the effectiveness of crosstalk reduction, i.e. at 1 kHz, the NEXT values of the HLS-TWP/TWP model are approximately between -140 and -150dB while the best value of those in the inset is approximately -120dB. The different performances of crosstalk suppression can be directly explained by Eq. (IVB-2). The source cancellation, due to the induced sources with opposite polarities on both sides of the twisted junction (B_n and A_{n+1}), causes the reduction of the induced voltage as discussed above. Simulations also showed that the multi-conductor transmission line based simulation is less consistent when the length of the cable is considered electrically long or when curves enter the frequency of standing-wave region at above 1 MHz for a 5.28-m long UTP-CAT5 cable.

The effects of using the balanced input technique are examined in the next simulation. The results are compared with those obtained by driving a single wire generator. The computed NEXT results on the receptor-wire pair 3-4 using the HLS-TWPD/TWP model are shown in Fig. IVB-4(b) when generator wires 1 and 2 are driven, respectively, by +0.5 V and -0.5 V sources. Compared with the results presented in Fig. IVB-4(a), one can see the further enhancement in crosstalk reduction in the region of 100 kHz to 10 MHz. In this case, the NEXT level depends less on the current and more on the difference of 'L_{G1}-L_{G2}' and '$L_{G'1}$-$L_{G'2}$', particularly for the 1-kΩ load impedance case. Another comparison is made with the plots shown in the inset where the associated crosstalk circuit models using the balanced input technique as discussed in a previous study (STD/STP, TWPD/TWP, and STD/TWP models in [22]). At 1 kHz, the NEXT values of the HLS-TWP/TWP model are approximately between -140 and -150dB while the best value in side the inset is approximately -130dB. The similar results can be

seen for the receptor-wire pairs 5-6 and 7-8 as the associated computed results are shown in Figs. IVB-4(c) and IVB-4(d), and IVB-4(e) and IVB-4(f), respectively, for both types of driving signals. Since the crosstalk circuit model used in this report considers no dielectric coating and no transmission-line loss, some discrepancy is expected between the analytical results and the EMT calculations. The EMT calculations take into account non-homogenous media and the current attenuation associated with the computer code-modeled UTP-CAT5 cable. The results suggest that the HLS-TWP/TWP and HLS-TWP/TWPD models are the most effective configurations in controlling the NEXT level, due to the influence coming from cancellation of the multiple sources on both sides of the twisted pair junction. For the final remark, it means if one makes a simple modification to the commercially available less expensive UTP-CAT5 cable by applying the half-loop shifting technique, it is possible to achieve a significant reduction in crosstalk, leading to much more acceptable levels of crosstalk for both the low and high load impedances.

Accomplishments:

One journal publication (Progress In Electromagnetics Research, PIER).

XI. SUMMARY OF EXPERIMENTS: SLOT APERTURE INTERACTION TESTS USING SEMI-ANECHOIC ELECTROMAGNETIC TEST CHAMBER

An AFOSR supplementary grant has enabled us to perform experiments to validate EMT based simulation results. The diagram and specification of the FS4010 system is shown in Fig. IVC-1. This system consists of the following; (i) RF amplifier, (ii) RF signal generator, (c) power meter, (d) RF system controller, (e) dual directional coupler, (f) isotropic E field probe, (g) current probes, (h) an anechoic test chamber, and (i) test accessories. Equipments are for the measurement of induced currents at different wiring of a network under electromagnetic excitation.

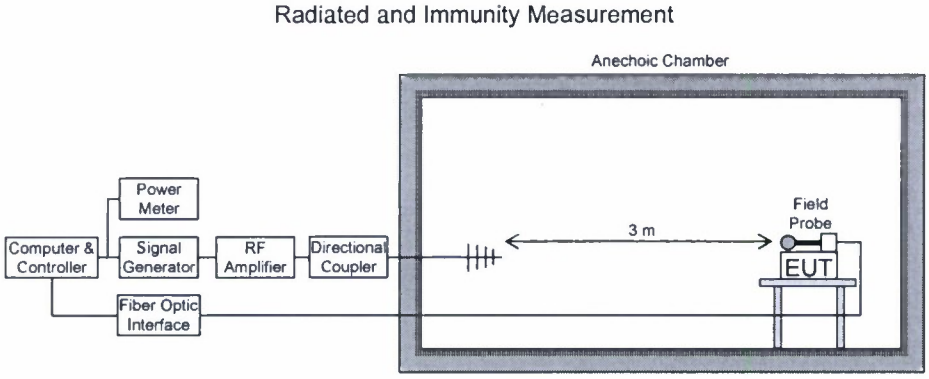

System Parameters

Frequency range	27 – 1000 MHz
Field strength	10 V / m max
Max DUT size	100 × 100 cm^2
Input RF power	150 Watts max
Cell dimension	5.7 × 2.6 × 2.4 m^3

Fig. 1VC-1 FS4010 system.

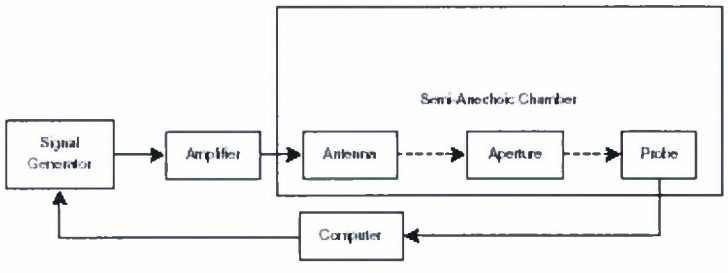

Fig. 1VC-2 Experiment setup.

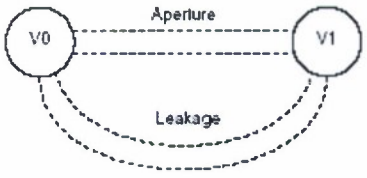

Fig. IVC-3 Experiment topology.

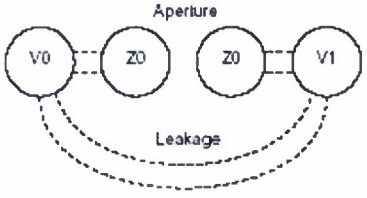

Fig. IVC-4 Experiment topology to isolate the leak.

The equipment available to perform the experiment was arranged according to Fig. IVC-2. Applying EMT to the semi-anechoic chamber yields the topological network shown in Fig. IVC-3. The aperture divides the chamber into two volumes that interact through the aperture and through leakage around the aperture. The transfer function equation for Fig. IVC-3 is $H_{ap}(\omega) + H_{leak}(\omega) = \dfrac{E_{trans,all}(\omega)}{E_{inc}(\omega)}$, (IVC-1)

where $H_{ap}(\omega)$ is the transfer function of the aperture, $H_{leak}(\omega)$ is the transfer function of the leak, $E_{inc}(\omega)$ is the incident electric field on the illuminated side of the aperture, and $E_{trans,all}(\omega)$ is the transmitted electric field on the shadowed side of the aperture. Since the leak cannot be removed or neglected, it must be measured. To isolate the leak, the aperture must be terminated in such a way that no energy penetrates or is reflected from it. This can be thought of as terminating the aperture with a load that resembles free-space. To accomplish this, the aperture was plugged with absorbing material used in the semi-anechoic chamber. The resulting topological network can be seen in Fig. IVC-4. The transfer function equation for Fig. IVC-4 is

$$H_{leak}(\omega) = \frac{E_{trans,leak}(\omega)}{E_{inc}(\omega)}, \qquad \text{(IVC-2)}$$

where $E_{trans,leak}(\omega)$ is the transmitted electric field on the shadowed side of the aperture. Substituting Eq. (IVC-2) into Eq. (IVC-1) yields

$$H_{ap}(\omega) = \frac{E_{trans,all}(\omega) - E_{trans,leak}(\omega)}{E_{inc}(\omega)}. \qquad \text{(IVC-3)}$$

A LabVIEW Virtual Instrument (VI) was created to automate the generation and measurement of electric fields in the semi-anechoic chamber. The name of the VI is "Aperture Constant Power" and takes the following inputs

Test File A text file containing the frequencies to generate.

Operator The name of the person performing the test.

Description A description of the test.

Signal Generator The GPIB address of the signal generator.

Probe The serial port connected to the probe.

Power The power output of the signal generator.

Desired Field Polarization The polarization of the antenna.

# of Points The number of samples taken from the probe and averaged to yield one measurement.

Dwell Time The number of milliseconds the system waits until sampling when changing frequencies.

The visible outputs to the user are

Current Frequency The current frequency being tested.

Progress A progress indicator.

E-Field A digital display of the current measured electric field in RMS volts per meter.

E-Field A chart showing recently measured electric fields.

Actual Incident A graph showing the XYZ components of the E-field versus frequency.

The VI also records the setup information and measured data in text file. The text file contains

Date The date of the test.

Time The time of the conclusion of the test.

Operator Same as above.

Description Same as above.

Power Same as above.

Dwell Time Same as above.

Polarization Same as above.

Data A locus of frequency, Ex, Ey, Ez pairs.

The VI works as follows

1. Parse the text file supplied by the user.
2. Initialize the signal generator.
3. Initialize the probe.
4. Set the power of the signal generator and then for each frequency listed, wait the dwell time, then take and average a number of samples from the probe.
5. Reset the signal generator.
6. Save the measured data to a text file.

The signal generator is a Rohde & Schwarz SML 01. It is rated for frequencies from 9kHz to 1.1GHz and power levels of –140 dBm to +13 dBm. The amplifier is an Amplifier Research 150W1000. The amplifier is rated for 150 W in the range between 80 MHz and 1 GHz. The semi-anechoic test chamber and built-in antenna is an Amplifer Research TC4000B. It's rated up to 500 W of input and frequencies between 27 MHz and 4.2 GHz. The useable volume in the chamber is 4-m deep, 1.8-m wide, and 2.15-m tall. The antenna can be rotated for vertical or horizontal polarizations. The electric field probe is an Amplifier Research FP7003. The probe is an isotropic probe rated for frequencies from 100 kHz to 3 GHz and field levels of .4 V/m to 660 V/m. The isotropic nature of the probe allows it to be physically rotated to correspond to a user-defined coordinate system. Since physically rotating the probe was not practical, the rotation was performed in software. One limitation of the probe is that fact that it only reports the effective electric field for each axis that it measures. This limitation prevents the determination of the phase angle of the aperture's transfer function. The aperture is a 6 ft by 4 ft by 1in aluminum frame holding two 4 ft by 2 ft by .125 inches pure aluminum sheets. The width between sheets is adjustable in two inch increments.

For most experiments, the following settings apply unless otherwise stated

- The gain setting of the signal generator was –15 dBm for the duration of the experiment.
- The amplifier gain was 100% for the duration of the experiment.
- The probe was configured for 60Hz, all-axes measurements.
- The dwell time was 500 ms.

- The number of samples used for averaging was 30.
- The antenna, probe, and aperture were setup for horizontal polarization.

For the experiment as the anechoic chamber and setup are shown in Fig. IVC-5, the aperture was placed 3 m from the antenna. The slot aperture widths used were 2, 6, 10, and 14 inches. The probe was placed 10, 20, 30, 40, and 50 cm behind the aperture for each aperture width. The frequencies used were from 80 MHz to 1 GHz spaced linearly in 10 MHz increments. The expected cut-off frequencies are listed in Table IVC-1. A typical trial (10-inch aperture, probe placed 10 cm behind) can be seen in Fig. IVC-6. The first observation that should be made from this graph is that the aperture does show high-pass filter characteristics. Both transmitted signals are attenuated at low frequencies while the un-plugged transmitted signal follows the incident signal at high frequencies. The second observation is that the foam plug performs well enough to show a significant change in signal. Both transmitted signals are close for low frequencies because the aperture is blocking them without the help of the foam. At higher frequencies, the aperture permits more signal through while the foam attenuates that signal.

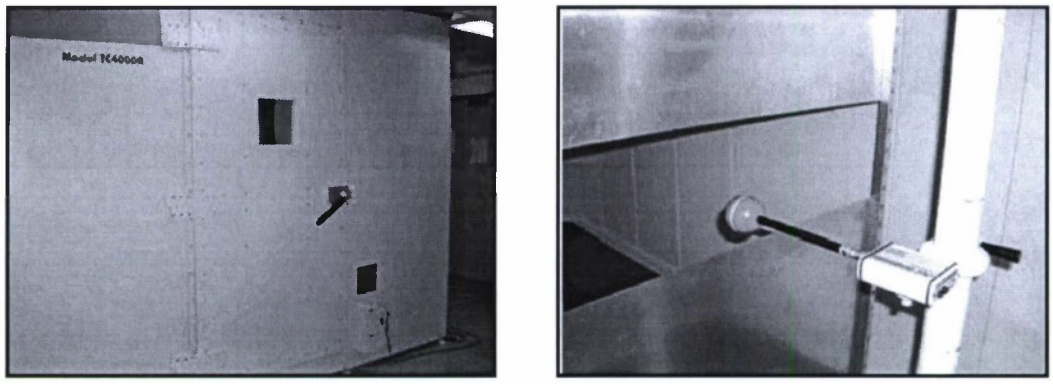

Fig. IVC-5 Anechoic chamber and equipment setup.

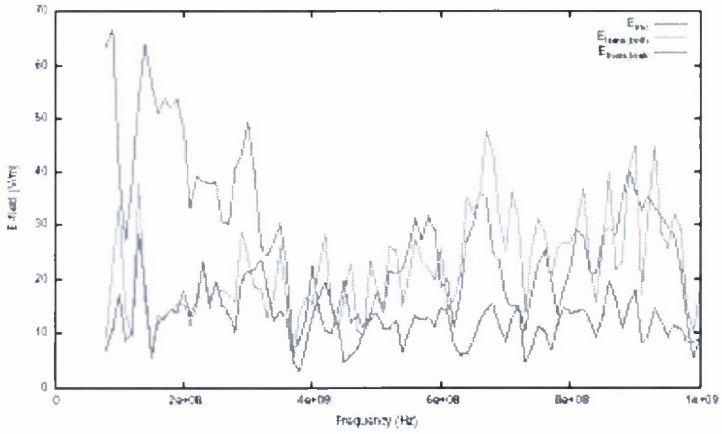

Fig. IVC-6 Typical trial.

All of the experimentally determined transfer functions are presented in Table IVC-2. The first observation is that the experimental curves tend to shift left with increasing aperture width. This is expected since the cut-off frequency for a wide aperture is lower than a narrow aperture. The second observation is that the curve shifts down as the probe is moved further from the aperture. This also is expected since a radiated signal decays with distance.

Table IVC-1 Aperture widths and associated cut-off frequencies.

w in	f_c MHz
2	2953
6	984
10	591
14	422

Table IVC-2 Measured transfer functions versus aperture width and probe distance.

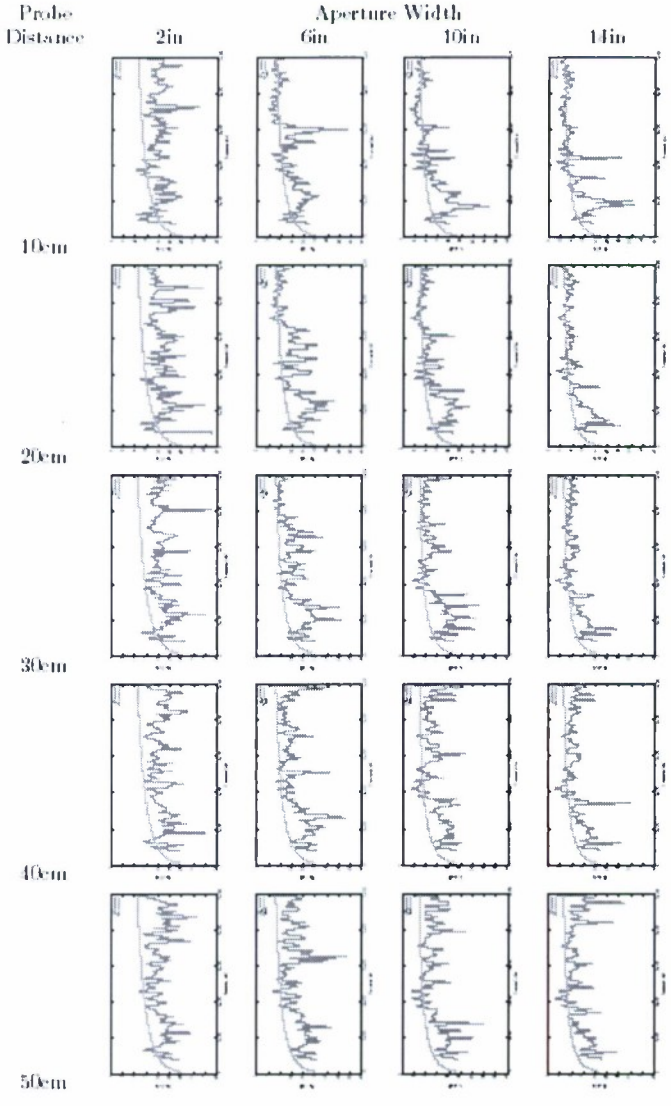

Accomplishments: To be use in future research and publications and projects.

XII. SUMMARY: TRAINING ON EMT BASED SIMULATION AND EXPERIMENTS

Training topic: Electromagnetic topological network simulations and applications using CRIPTE code

HiPER Laboratory, University of Missouri-Columbia, Aug 23 – 24, 2006.

During August 2006, the HiPER laboratory offered a two-day training course on electromagnetic topology simulations and applications to Dr. Robert Kipp, a chief scientist from Delcross Technologies, Chicago, Illinois as a part of AFRL collaboration to compare a performance of the BLT equation-based simulations in frequency domain (CRIPTE code) and in time domain. This project is also funded by SBIR through AFSOR and is under supervision of Dr. Frederick Tesche (EMConsultant, Fairview, NC) and Dr. Eric Michielssen (ECE department, University of Michigan).

The training course content includes:

1. Application to an aircraft system
2. A network for each shielding level
3. Simulation scheme
4. Tube (per unit length parameters L, C, R, G)
5. Junction (impedances and S-parameters)
6. Source (external and internal couplings)
7. Other applications and modeling examples.

XIII. REFERENCES

1. H. A. Bethe, "Theory of diffraction by small holes," Phys. Rev., vol. 66, pp. 163-182, 1994.
2. C. M. Butler, Y. Rahmat-Samii, and R. Mittra, "Electromagnetic penetration through apertures in conducting surfaces," IEEE Trans. Electromagn. Compat., vol. EMC-20, no. I, pp. 82-93, Feb. 1978.
3. J. P. Parmantier, V. Gobin, F. Issac, I. Junqua, Y. Daudy, and J. M. Lagarde, "An application of the electromagnetic topology theory on the test-bed aircraft, EMPTAC," Interaction Notes 506, Kirtland, 1993.
4. C. E. Baum, "Electromagnetic Topology : A formal approach to the analysis and design of complex electronic systems," Interaction Notes 400, Kirtland, 1980; also in Proc. Zurich EMC Symp., 209-214, 1981.
5. F. M. Tesche, "Topological concepts for internal EMP interaction," IEEE Trans. Electromagn. Compat., vol. EMC-20, no. 1, pp. 60-64, Feb. 1978.
6. Model Development and Verification of the CRIPTE code for Electromagnetic Coupling, FINAL REPORT, AFOSR Grant F49620-02-1-0183, April 2002-October2005.
7. P. Kirawanich, N. Kranthi and N. E. Islam, "Electromagnetic topology based analysis of coupling through small aperture on cables of communication systems," Electromagnetics, vol. 25, no. 7-8, pp. 589 602, Oct.-Dec. 2005.
8. J. E. Nanevicz, E. F. Vance, W. Radasky, M. A. Uman, G. K. Soper, and J. M. Pierre, "EMP susceptibility insights from aircraft exposure to lightning," IEEE Trans. Electromagn. Compat., vol. 30, no. 4, pp. 463-472, Nov. 1988.
9. CRIPTE user's manual: research version. 2003.
10. K. S. H. Lee, EMP Interaction: Principles, Techniques and Reference Data, Bristol, PA: Hemisphere, 1986.
11. S. J. Orfanidis, Electromagnetic Waves and Antennas, on-line version text book.
12. K. S. Yee, "Numerical solution of initial boundary value problems involving Maxwell's equations in isotropic media," IEEE Trans. Antennas Propagat., vol. AP-14, no. 3, pp. 302-307, May 1966.
13. S. Celozzi and M. Feliziani, "EMP-coupling to twisted-wire cables," IEEE Int. Symp. on EMC, Washington, DC, USA, Aug. 21–23, 1990.
14. Maki, M., et al., "Home information wiring system using UTP cable for IEEE 1394 and Ethernet systems," IEEE Trans. Consumer Electron., Vol. 47, No. 4, pp. 921–927, 2001.
15. C. R. Paul and J. W. McKnight, "Prediction of crosstalk involving twisted-pairs of wires-part I: a transmission-line model for twistedwire pairs," IEEE Trans. Electromagn. Compat., Vol. EMC-21, No. 2, pp. 92–105, 1979.
16. C. R. Paul and J. W. McKnight, "Prediction of crosstalk involving twisted-pairs of wires-part II: a simplified lowfrequency prediction model," IEEE Trans. Electromagn. Compat., Vol. EMC-21, No. 2, pp. 105–114, 1979.
17. G. R. Piper and A. Prata, Jr., "Magnetic flux density produced by finite-length twisted-wire pairs," IEEE Trans. Electromagn. Compat., Vol. 38, No. I, pp. 84–92, 1996.
18. C. D. Taylor and J. P. Castillo, "On the response of a terminated twisted-wire cable excited by a plane-wave electromagnetic field," IEEE Trans. Electromagn. Compat., Vol. EMC-22, No. 1, pp. 16–19, 1980.
19. IEEE 802.3 Working Group, IEEE Standard 802.3u 1995Ed. (Supplement to ISO/IEC 8802-3: 1993; ANSI/IEEE Std 802.3, 1993 Ed.).
20. C. E. Baum, Interaction Notes 478, Kirtland, New Mexico, USA (1989).
21. J. P. Parmantier and J. P. Aparicio, "Electromagnetic topology: coupling of two wires through an aperture," Int. Zurich EMCSymp., Zurich, Switzerland, March 12–14, 1991.
22. P. Kirawanich, N. E. Islam, and S. J. Yakura, "An electromagnetic topological approach: crosstalk characterization of the unshielded twisted-pair cable," Progress In Electromagnetics Research, PIER 58, pp. 285–299, 2006.
23. C. Eswarappa, G. I. Costache, and W. J. R. Hoefer, "Transmission line matrix modeling of disperse wide-band absorbing boundaries with time-domain diakoptics for S-parameter extraction," IEEE Trans. Microwave Theory Tech., Vol. 38, No. 4, pp. 379-386, 1990.

XIV. PERSONNEL SUPPORTED

1. Phumin Kirawanich (Postdoctoral Fellow, INS permission to work in US)
   List of fully (2PhD students) and partially funded (summer/semester) personnel include the following
2. Rahul Gunda (Graduated)
3. Nakka S. Kranthi (Graduated)
4. Sravanthi Kache (Graduated)
5. Jeffery C. Kroenung (US national)
6. Andrew R. Stillwell (US national)
7. 6. Ryan Furtado (US national)
8. 7. George Ball (US national)
9. 8. Tim Evans (US national)
10. David S. Gleason (US national)
11. Robert Feldhaus (US national)
12. Ben (US national)
13. David Mueller (US national)
14. Justin Ross (US national)
15. Gena Belgarde(US national)
16. Ashkan Seyedi (US national)
17. Anthony Cornell (US national)
18. Waseem Akbar (unsupported)
19. Mohammad O. Nizam (resident alien)
20. Pavan K. Gummadavalli (unsupported)
21. Nikhil Parsi (unsupported
22. D. Sleper (collaborator, Professor, US citizen)
23. M. S. Pathan (collaborator, Research Associate, US citizen)
24. Bruno Camps-Raga (Ph.D. Student)
25. N. Boriraksantikul (Graduate Student)
26. N. Parsi (Graduate Student)
27. S. Tantong (Ph.D. Student)
28. S. R. Gyawali (Graduate Student).
29. Akeed A. Pavel (PhD student, Research Assistant)
30. Justin R. Wilson (US citizen)
31. Junior Students (US citizen)
    Bradley Collier, Eddie Griesenauer, Tony Mullen, Kevin Sprague, and Chris Wuebker, Project Supported: "Microwave Studio Simulation: High Power Electromagnetic Radiation Laboratory".
32. Students for Dr. Mahmoud Almasri use Microwave Studio Lab as a collaborative research project.

XV. PUBLICATIONS

Journal Publications

[2008J1] P. Kirawanich, S. J. Yakura, and N. E. Islam, "Simulating large electrical systems for wideband pulse interactions using the topological modular junction concept," IEEE Transactions on Plasma Sciences, vol. 36, no. 2, pp. 435-442, Apr. 2008 (invited paper).

[2007J1] Phumin Kirawanich, Justin R. Wilson, S. Joe Yakura, and N. E. Islam, "A generic topological simulation scheme for studying aperture electromagnetic field interactions and cable couplings," Journal of Applied Physics, vol. 102, pp. 024902(1-8), 2007.

[2007J2] Phumin Kirawanich, Justin R. Wilson, S. Joe Yakura, Christos Christodoulou, and N. E. Islam, "A modular junction topological approach to aperture - system interaction problem," IEEE Antennas and Wireless Propagation Letters, vol. 6, pp. 296-299, 2007.

[2007J3]Phumin Kirawanich, Nakka S. Kranthi, Rahul Gunda, Jean-Philippe Parmantier, Solange Bertuol, and N. E. Islam, Simulating the response of semi-shielded systems: electromagnetic topology technique, Ultra-Wideband Short-Pulse Electromagnetics 7, Kluwer Academic Publishers, expected 2007

[2006J1] P. Kirawanich, N. E. Islam, and S. J. Yakura, "An electromagnetic topology approach: crosstalk characterizations of the unshielded twisted-pair cable," *Progress In Electromagnetics Research*, J. A. Kong (ed.), PIER 58, pp. 285-299, 2006.

[2006J2] Rahul Gunda, David Gleason, Kapil Kelkar, Phumin Kirawanich, William C. Nunnally, and N. E. Islam, "Radiofrequency heating of photoconductive switch for high power applications," *IEEE Transactions on Plasma Sciences*, the 2006 special issue (submitted).

[2006J3] P. Kirawanich, D. Gleason, and N. E. Islam, "An electromagnetic topology and transmission line hybrid solution to aperture interactions," *Journal of Applied Physics* (revised).

[2006J4] Sravanthi Kache, Nakka S. Kranthi, M. O. Nizam, Phumin Kirawanich, R. W. McLaren, A. K. Sharma, S. L. Lucero, and N. E. Islam, "Field analysis to optimize charge collection in a sub-micron grated metal-semiconductor-metal photodetector," *Journal of Applied Physics* (submitted).

[2006B1] Phumin Kirawanich, Nakka S. Kranthi, Rahul Gunda, Jean-Philippe Parmantier, Solange Bertuol, and N. E. Islam, Simulating the response of semi-shielded systems: electromagnetic topology technique, Ultra-Wideband Short-Pulse Electromagnetics 7, Kluwer Academic Publishers, 2006.

[2005J1] Nakka S. Kranthi, M. O. Nizam, Phumin Kirawanich, Naz E. Islam, A. K. Sharma, and S. L. Lucero, "Fields analysis of enhanced charge collection in nanoscale grated photo detectors," *Applied Physics Letters* , vol. 87, no. 24, Dec. 2005.

[2005J2] Phumin Kirawanich, Nakka Kranthi and N. E. Islam, "Electromagnetic topology based analysis of coupling through small aperture on cables of communication systems," *Electromagnetics*, the special issue on "RF Effects on Digital Systems: Part I", vol. 25, no. 7-8, pp. 589-602, Oct.-Dec. 2005.

[2005J3] Phumin Kirawanich, George Tzeremes, Christos Christodoulou, S. Joe Yakura, and N. E. Islam, "Electromagnetic wave penetrating through apertures: Comparison of electromagnetic

topology technique with FDTD method," *Antennas and Wireless Propagation Letters*, vol. 4, no. 15 , pp. 151-154, 2005.
[2005B1] F. J. Agee, P. Kirawanich, J. Yakura, G. Tzeremes, C. Christodoulou, and N. E. Islam, An electromagnetic topology based simulation for aperture interactions using transmission lines as radiating elements, Computational Methods and Experimental Measurements XII, Wessex Institute of Technology Transactions on Modelling & Simulation (ISSN 1743-355X), vol 41, pp. 94, 2005.

Reviewed Conference Proceedings

[2008C1] D. Sleper, M. S. Pathan, B. Camps-Raga, N. Boriraksantikul, S. Tantong, S. R. Gyawali, P. Kirawanich, and N. E. Islam, "Experimental Analysis of Corn Seed Germination Enhancement under the Application of Electromagnetic and Magnetic Fields," EUROEM-2008, July 21-25, 2008, Lausanne, Switzerland.

[2008C2] B. Camps-Raga, P. Kirawanich, N. E. Islam, and C. E. Baum, "Topological Cell Model For Energy Transmission in a Cuvette," Proceeding of the 2008 IEEE International Conference on Plasma Science, ICOPS 2008, 15-19 June 2008, Karlsruhe, Germany.

[2008C3] N. Parsi, S. R Gyawali, N. Boriraksantikul, P. Kirawanich, N. E. Islam, M. S. Pathan, and D. Sleper "Improving Germination Rate of Soybeans as a Biofuel Resource," Proceeding of the 2008 IEEE International Conference on Plasma Science, ICOPS 2008, 15-19 June 2008, Karlsruhe, Germany.

[2008C4] B. Camps-Raga, N. Boriraksantikul, P. Kirawanich, W. C. Nunnally, and N. E. Islam, "Characterizing a Transverse Electromagnetic Cell with Nanosecond Pulsed Electric Fields for Biological Applications," Proceeding of the 2008 IEEE International Power Modulator Conference, IPMC 2008, 27-31 May 2008, Las Vegas, Nevada, USA.

[2008C5] N. Boriraksantikul, P. Kirawanich, and N. E. Islam, "Electromagnetic Radiation Study of Commercial Cellular Phones with a TEM Cell for Biological Applications," Proceedings of the 2008 IEEE Region 5 Technical, Professional, and Student Conference, Apr. 17-20, 2008, Kansas City, Missouri, USA.

[2007C1] Phumin Kirawanich, James E. Thompson, and Naz E. Islam, "A Modular Junction Topological Approach to System Interaction Problems: Simulation and Validation," Proceedings of the 18th International Zurich Symposium on Electromagnetic Compatibility, Sep. 24-28, 2007, Munich, Germany.

[2007C2] Phumin Kirawanich, Christos Christodoulou, Justin R. Wilson, S. Joe Yakura, and N. E. Islam, "Electromagnetic Topology: a Modular Junction Approach for a System Level Interaction Problem," Presentation and Proceedings of the 2007 IEEE Electromagnetic Compatibility Symposium, July 8-13, 2007, Honolulu, Hawaii, USA.

[2007C3] P. Kirawanich, S. J. Yakura, and N. E. Islam, "Study of a Wideband Pulse Interaction on a Large System Using a Modular Junction Topological Approach," Proceeding of the 2007 IEEE Pulsed Power and Plasma Science Conference, PPPS 2007, 17-22 June 2007, Albuquerque, New Mexico, USA.

[2006C1] S. J. Yakura, Phumin Kirawanich, Justin R. Wilson, and N. E. Islam, "Aperture analysis through electromagnetic topology: simulations and experimental validation," the Ninth Annual Directed Energy Symposium, Albuquerque, New Mexico, Oct 30 – Nov 2, 2006.

[2006C2] S. J. Yakura, P. Kirawanich, and N. E. Islam, "Crosstalk characterizations of unshielded twisted-pair cables," the 2006 the DEPS Joint UK/US High Power Microwave (HPM) Conference HPM conference, Adelphi, Maryland, Apr 3-6, 2006.

[2006C3] Phumin Kirawanich, S. Joe Yakura, and N. E. Islam, "Electromagnetic Topology Simulations for Cable Coupling with a Radiating Dipole at an Aperture," the 2006 IEEE EMC Symposium, Portland, Oregon, Aug 14-18, 2006.

[2006C4] Justin R. Wilson, Phumin Kirawanich, and N. E. Islam, "Integration of Electromagnetic Topology Concept and Measurement for High Power Radio-Frequency Interaction Study," AMEREM Meeting, Albuquerque, New Mexico, USA, July 9-14, 2006.

[2006C5] Phumin Kirawanich, S. Joe Yakura, and N. E. Islam, "Electromagnetic Topology Simulations for Cable Coupling with a Radiating Dipole at an Aperture," the 2006 IEEE EMC Symposium, Portland, Oregon, Aug 14-18, 2006.

[2006C6] Justin R. Wilson, Phumin Kirawanich, and N. E. Islam, "Integration of Electromagnetic Topology Concept and Measurement for High Power Radio-Frequency Interaction Study," AMEREM Meeting, Albuquerque, New Mexico, USA, July 9-14, 2006.

[2006C7] Phumin Kirawanich, David Gleason, S. Joe Yakura, and N. E. Islam, "Crosstalk characterizations of an unshielded twisted-pair cable in an electrical large system using the electromagnetic topology concept," Proceedings of the 17th International Zurich Symposium on Electromagnetic Compatibility, Feb. 27- Mar. 03, 2006, Singapore.

[2005C1] S. Joe Yakura, Phumin Kirawanich, David Gleason, and N. E. Islam, "Application of transmission line matrix methodology to electromagnetic topology simulations for EMP penetration through apertures," the International Conference on Electromagnetics in Advanced Applications and European Electromagnetic Structures Conference, ICEAA '05 and EESC '05, Sep. 12-16, 2005, Torino, Italy.

[2005C2] Phumin Kirawanich, David Gleason, Anthony Cornell, and N. E. Islam, "Analysis of field through apertures by applying transmission line matrix method to electromagnetic topology simulations," Proceedings of the 2005 IEEE Electromagnetic Compatibility Symposium, Aug. 8-12, 2005, Chicago, Illinois, USA.

[2005C3] Phumin Kirawanich, David Gleason, and N. E. Islam, "Simulations for high power microwave penetration through apertures: application of transmission line matrix methodology to electromagnetic topology," Abstract at the 32nd IEEE International Conference on Plasma Science, ICOPS 2005, 18-23 June 2005, pp. -, Monterey, California, USA.

[2005C4] Rahul Gunda, Phumin Kirawanich, and N. E. Islam, "Effects of heating on Photoconductive Semiconductor switches: simulation and analysis," Proceeding of the 15th IEEE International Pulsed Power Conference, PPC 2005, 13-17 June 2005, pp. -, Monterey, California, USA.

[2005C5] Phumin Kirawanich, David Gleason, and N. E. Islam, "An electromagnetic topology and transmission line matrix hybrid technique for modeling high power electromagnetic interactions," Proceeding of the 15th IEEE International Pulsed Power Conference, PPC 2005, 13-17 June 2005, pp. -, Monterey, California, USA.

[2005C6] Forrest J. Agee, Phumin Kirawanich, S. Joe Yakura, George Tzeremes, Christos Christodoulou, and N. E. Islam, "An electromagnetic topology based simulation for aperture interactions using transmission lines as radiating elements," 12th International Conference on Computational Methods and Experimental Measurements (CMEM 2005), 20-22 June 2005, Malta.

[2005C7] Phumin Kirawanich, Nakka S. Kranthi, A. R. Stillwell, Forrest J. Agee, S. Joe Yakura, and N. E. Islam, "Analysis of the wire coupling under an aperture illuminated by an incident field by means of a topological approach," Proceedings of the 16th International Zurich Symposium on Electromagnetic Compatibility, Feb. 13-18, 2005, Zurich, Switzerland.

XVI. INTERACTIONS/TRANSITIONS

Conferences, meetings, and symposium

We have actively participated in several EMC-related symposiums, meetings and conferences, and contributed by giving presentation. Besides the US conferences and presentations we have participated in the following international events and have familiarized a worldwide audience in the concept of EMT simulation methods. Some of our work has been presented in classified presentation (shown below) through our collaborators at AFRL/NM.

Classified Presentation

The Five-power Air Senior National Representative (ASNR) High Power Microwave Meeting, held 14-17 February 2005 at Eglin AFB, FL. The meeting is held every six months either in the US or Europe, alternating the location every six months. The five-power nations consist of the senior government officials from USA, the UK, Germany, France and Italy. Since Italy just became a member last year, Italy has not yet sent anybody to the meeting. The purpose of this group is to share the information and establish international collaboration on HPM research among participating nations.

- The title of the paper presented is "Analysis of the Wire Coupling under an Aperture Illuminated by an Incident Field by Means of a Topological Approach."
- The paper was presented by S. Joe Yakura (AFRL/DEHE) and coauthors included N. E. Islam and Forrest J. Agee (AFOSR) amongst others.

The Ninth Annual Directed Energy Symposium, held Oct 30 – Nov 2, 2006 at Kirtland, AFB, New Mexico. The meeting is organized and sponsored by Directed Energy Professional Society (DEPS) and Air Force Research Laboratory Directed Energy Directorate. The Ninth Annual Directed Energy Symposium will bring together researchers, managers, and policy makers from government offices, DoD, DoE, and other national laboratories, program offices, the intelligence community, industry, universities, and other scientific and engineering institutions for discussions of current programs, technology efforts, and the future of Directed Energy. This annual Symposium provides a forum for the exchange of technical information in fields related to the development, testing, and fielding of High Energy Laser (HEL) and High Power Microwave (HPM) systems. One special feature of this Symposium is that no limited distribution sessions are being planned. All Symposium events will be either open or classified.

- The title of the paper presented is "Aperture analysis through electromagnetic topology: simulations and experimental validation".
- The authors are S. Joe Yakura (AFRL/DEHE), Phumin Kirawanich (U of Missouri at Columbia), Justin R. Wilson (U of Missouri at Columbia), and N. E. Islam (U of Missouri at Columbia).

The Directed Energy Professional Society (DEPS) Joint UK/US High Power Microwave Conference (classified), held Apr 3-6, 2006 at Adelphi, Maryland. The meeting is organized and sponsored by Directed Energy Professional Society (DEPS) and Army Research Laboratory.

This conference covers the progress in the development and application of high power microwave (HPM) technologies for directed energy missions was explored in this conference, specifically devoted to HPM. This conference was classified SECRET with participation limited to U.S. and U.K. attendees with appropriate security clearances.

- Paper title "Crosstalk characterizations of unshielded twisted-pair cables".
- Authors are S. Joe Yakura (AFRL/DEHE), P. Kirawanich (Univ. of Missouri at Columbia), and N. E. Islam (Univ. of Missouri at Columbia).

Directed Energy Professional Society (DEPS) High Power Microwave Conference (classified), held 17-19 August 2004 in Albuquerque, NM. This conference covers the progress in the development and application of high power microwave (HPM) technologies for directed energy missions. It suggests that it is time for DEPS to sponsor a conference specifically devoted to HPM. Re-establishment of a common perspective on HPM missions and potential directions requires the appropriate security level and the attendance of the relevant experts and managers. This conference is classified SECRET. Attendance was limited to U.S. citizens with secret or higher security clearances.

- Paper title "Approximated Non-uniform Baum-Liu-Tesche (BLT) Formulation of Transmission-line Theory for One-wire Network Systems."
- Authors are S. Joe Yakura (AFRL/DEHE) N. E. Islam (Univ. of Missouri at Columbia) and P. Kirawanich (Univ. of Missouri at Columbia).

Consultative and advisory functions to laboratories and agencies

We have established close, interactive research collaboration with the Directed Energy Directorate, AFRL, NM. We have also collaborated with Space Vehicles Directorate in the device analysis areas, specifically in radiation effects studies. Our interactions with AFRL/DE include frequent exchange of information regarding usage and models for the CRIPTE code and the producing joint collaborative technical papers for both Conferences and to Journals. Our collaborators also include the Electrical and Computer Engineering Department, University of New Mexico and the Center for High Technology Materials (CHTM), UNM. At the Directed Energy Directorate, our principal collaborators include Dr. Joe Yakura and Bill Prather. A number of research papers include collaborative authors from UNM (Dr. Christos Christodolou, Dr. Karl Baum) and Dr. Joe Yakura (AFRL/NM)

Whenever required we have provided the necessary help for the AFRL group to understand the inner workings of the code and have consulted the group to setup small scale experiments at U Missouri-Columbia. Experiments will be conducted at the U Missouri-Columbia laboratories.

Transitions

i) We have started interactions with Dr. Robert Kipp, a chief scientist from Delcross Technologies, Chicago, Illinois. It is a part of AFRL collaboration with SBIR clients to develop a simulation code based on the BLT equation in time domain. We expect to use the code for time domain analysis in collaboration with AFRL for future research. The simulation performance will also be evaluated and compared with simulations using the CRIPTE code in frequency domain.

ii) In a technical exchange meeting between the 46 Test Wing and Air Armament Center personnel at Eglin AFB, FL, and AFRL/KAFB, NM, the use of the CRIPTE code at

AFRL/DEHE for high power microwave effects studies was discussed where presentation was done of our work by Dr. Yakura.

iii) The techniques we have established for external-internal interactions through an aperture for EMC/EMI studies can be utilized for aircraft cable or other sensitive military hardware. We expect Dr. Yakura at DE/AFRL, NM to conduct research in this area.

iv) This research has the potential to contribute to any DoD research where electromagnetic interactions with large systems is the objective of study. Conventional techniques can be mixed and matched with the EMT techniques proposed to modularly solve individually, which can be later integrated to the full volume which describes the system.

XVII.NEW DISCOVERIES

Electrically large systems are difficult to simulate using conventional simulation tools because of the large number of mesh points required. As a result the effort is cumbersome, time consuming and impractical. We have reported, for the first time, that a modified simulation scheme known as electromagnetic topology (EMT) method can be a good substitute for very large systems. Important discoveries that we have reported in the EMT simulation method includes:
1. A technique to generate the transfer function for the topological simulation network, which is generated by considering short circuited radiating dipoles and loop antennas at the aperture that behaves consistently as a high-pass filter with a cutoff frequency for a near-field region. This method can replace the experimentally determined values that was required previously.

2. We propose a simpler and accurate methodology, which combines the EMT approach with the transmission line matrix (TLM) method to account for the coupling of an incident electromagnetic field with an aperture over an infinite metallic plane in a topological simulation setting.
3. Based on EMT analysis, the straight-through, differential-generator, twisted-pair receptor model is the most effective configuration to control the near-end crosstalk level, due to the influence from both the neutralizing mutual inductance and the single current generator.
4. We have reported, for the first time, the half-loop shifting technique to achieve a significant reduction in unshielded twisted-pair cable crosstalk. This technique leads to much more acceptable levels of crosstalk for both the low and high load impedances with a simple modification to the commercially available less expensive.

XVIII. HONORS/AWARDS

1. Research presented at special (closed) meetings through our AFRL/NM collaborators.
2. Was nominated for and granted IEEE senior membership for recent accomplishments which including research work for the AFOSR supported project.
3. Recipient of research a supplement research grant of $173,000 for the test chamber to perform an electromagnetic conducted and radiation susceptibility tests.

ACKNOWLEDGEMENT

We sincerely acknowledge the advice and support extended to us by Dr. Joe Yakura, Bill Prather, and Dr. Mike Harrison at DEHE, AFRL, NM.

Thanks are also due to AFOSR Program Manager, Dr. Robert Barker, for his confidence and support for our effort which has lead to the establishment of a simulation and experimental facility to study the effects of electromagnetic fields on electrical systems as well as on life science.